In vitro evaluation of organic extractable matter from ambient PM2.5 using human bronchial epithelial BEAS-2B cells: Cytotoxicity, oxidative stress, pro-inflammatory response, genotoxicity, and cell cycle deregulation

Imane Abbas, Ghidaa Badran, Anthony Verdin, Frédéric Ledoux, Mohamed Roumie, Jean-Marc Lo Guidice, Dominique Courcot, Guillaume Garçon

IN VITRO EVALUATION OF ORGANIC EXTRACTABLE MATTER FROM AMBIENT $PM_{2.5}$ USING HUMAN BRONCHIAL EPITHELIAL BEAS-2B CELLS: CYTOTOXICITY, OXIDATIVE STRESS, PRO-INFLAMMATORY RESPONSE, GENOTOXICITY, AND CELL CYCLE DEREGULATION.

Imane ABBAS[1,#], Ghidaa BADRAN[1,2,3, #], Anthony VERDIN[2], Frédéric LEDOUX[2], Mohamed ROUMIE[1], Jean-Marc LO GUIDICE[3], Dominique COURCOT[1], Guillaume GARÇON[3,*]

[1] Lebanese Atomic Energy Commission – NCSR, Beirut, Lebanon;

[2] Unité de Chimie Environnementale et Interactions sur le Vivant, UCEIV EA4492, FR CNRS 3417, Univ. Littoral Côte d'Opale, Dunkerque, France;

[3] CHU Lille, Institut Pasteur de Lille, EA4483-IMPacts de l'Environnement Chimique sur la Santé Humaine (IMPECS), Univ. Lille, Lille, France.

[#] Both authors equally contributed and should be considered as co-first authors

Corresponding Author: Guillaume GARÇON, EA4483-IMPacts de l'Environnement Chimique sur la Santé Humaine (IMPECS), Institut Pasteur de Lille, CHU Lille, Univ. Lille, Lille, France, Phone number: +33-320626818, E-mail: guillaume.garcon@univ-lille.fr.

ABSTRACT

A particular attention has been devoted to the type of toxicological responses induced by particulate matter (PM), since their knowledge is greatly complicated by the fact that it is a heterogeneous and often poorly described pollutant. However, despite intensive research effort, there is still a lack of knowledge about the specific chemical fraction of PM, which could be mainly responsible of its adverse health effects. We sought also to better investigate the toxicological effects of organic extractable matter (OEM) in normal human bronchial epithelial lung BEAS-2B cells. The wide variety of chemicals, including PAH and other related-chemicals, found in OEM, has been rather associated with early oxidative events, as supported by the early activation of the sensible NRF-2 signaling pathway. For the most harmful conditions, the activation of this signaling pathway could not totally counteract the ROS overproduction, thereby leading to critical oxidative damage to macromolecules (lipid peroxidation, oxidative DNA adducts). While NRF-2 is an anti-inflammatory, OEM exposure did not trigger any significant change in the secretion of inflammatory cytokines (*i.e.*, TNFα, IL-1β, IL-6, IL-8, MCP-1, and IFNγ). According to the high concentrations of PAH and other related organic chemicals found in this OEM, *CYP1A1* and *1B1* genes exhibited high transcription levels in BEAS-2B cells, thereby supporting both the activation of the critical AhR signaling pathway and the formation of highly reactive ultimate metabolites. As a consequence, genotoxic events occurred in BEAS-2B cells exposed to this OEM together with cell survival events, with possible harmful cell cycle deregulation. However, more studies are required to implement these observations and to contribute to better decipher the critical role of the organic fraction of air pollution-derived $PM_{2.5}$ in the activation of some sensitive signaling pathways closely associated with G1/S and intra-S checkpoint blockage, on the one hand, and cell survival, on the other hand.

Keywords: organic extractable matter; BEAS-2B cells; oxidative stress; inflammation; genotoxicity; cell survival

1 - INTRODUCTION

Nowadays, air-pollution-derived particulate matter (PM) is fully acknowledged to be a major public health problem, responsible for several hundreds of thousands of premature deaths and the loss of millions of dollars yearly in health care (AQiE 2016). Fine fraction of the PM (particles with an aerodynamic diameter $\leq$ 2.5 µm, $PM_{2.5}$) generally corresponds to a very complex and heterogeneous mixture of both inorganic and organic chemicals, from natural and anthropogenic sources, and its composition varies as a function of location and season depending on the diversity of sources and the effects of atmospheric processes (Abbas *et al.* 2018). Due to its size, $PM_{2.5}$ constitutes a serious health hazard. After its penetration, deposition and absorption deeply in the tracheobronchial and alveolar regions, it can also either exert its toxicity within the lungs or, after its translocation through the bronchoalveolar barrier, be distributed through the blood circulation into the whole body (Cao *et al.* 2014; Liu *et al.* 2016; Pui *et al.* 2014; Van Winkle *et al.* 2015). Epidemiological studies have shown a significant correlation between long-term exposure to $PM_{2.5}$ and the initiation and/or exacerbation of a wide range of adverse health effects, including asthma, chronic obstructive pulmonary disease, lung cancer, other respiratory and cardiovascular diseases, and premature death (Kim *et al.* 2016; Weber *et al.* 2016; Xing *et al.* 2016). In 2013, the international agency for research on cancer (IARC) has classified outdoor air pollution and its fine fraction as carcinogenic to humans, based on sufficient evidence of carcinogenicity in humans and experimental animals (Loomis *et al.* 2013).

Over the last two decades, *in vitro* toxicology methods have been heavily used as they constitute a relevant approach for determining and describing the underlying mechanisms involved in the toxicity triggered by air pollution-derived $PM_{2.5}$, at cellular and molecular scales. However, despite intensive research effort, there is still a lack of knowledge about the specific chemical fraction within airborne $PM_{2.5}$, which could be mainly responsible of its adverse effects on human health. A particular attention has also been devoted to the type of toxicological responses induced by PM, since this knowledge is greatly complicated by the fact that PM is generally a very complex and heterogeneous, regrettably often poorly described, pollutant (Perrone *et al.* 2013). Hence, a great deal of effort has been done to identify some characteristic patterns of *in vitro* toxicological responses which could be specifically related to airborne PM. In this respect, Lonkar and Dedon (2010) supported the current hypothesis that airborne PM with higher participation of crustal elements was predominantly associated with some molecular and cellular effects participating in severe health processes like chronic inflammatory lung diseases. Moreover, PM with larger anthropogenic participation may have a higher impact on lung and systemic cardiovascular diseases, due to its stronger oxidative and proinflammatory potentials. Gualtieri *et al.* (2010) and Perrone *et al.* (2013) reported that some coarse PM showing the presence of crustal elements, ions and metals, contributed to oxidative stress and, thereafter, inflammation, but, on the contrary, other coarse PM triggered inflammation through a reactive oxygen species (ROS)-independent pathway, as ROS levels were not significantly altered. Their results pertinently supported the growing evidence that PM-size, composition and origin interact in an intriguing manner together with the own responsiveness of the cell models to induce the adverse health effects of airborne PM. Hence, while the inclusion of inorganic constituent grouping provided useful information about the differential effects of PM components and sources, it is worthy to extend such approach to organic constituents. Towards this end, Delfino *et al.* (2010) stated that, despite a higher presence of metals within fine and quasi-ultrafine particles, polycyclic aromatic hydrocarbons (PAH) were the major redox-active components, and thereafter, inflammatory response inducers. Longhin *et al.*

(2013) indicated that low doses of $PM_{2.5}$ with high quantities of PAH induced an early cell cycle arrest with a subsequent inhibition of cytokinesis and, an induction of DNA damage. Against this background, Dergham *et al.* (2012, 2015) have already intended to gain information on the toxicological effects induced by chemical variations of airborne $PM_{2.5}$ samples produced during different seasons in rural-, urban-, or industrial-surroundings. Taken together, their results clearly supported that some inorganic, ionic and organic components can act as exogenous source of ROS and the possible role of other factors that remain to be determined (*e.g.*, interaction of $PM_{2.5}$ physical characteristics and cell uptake efficiency, role of other non-investigated chemicals and/or biological materials). Accordingly, PM contains a wide variety of organic chemicals, which could, directly or indirectly, through their metabolic activation, possibly participate to the induction of oxidative and/or proinflammatory events in human bronchial epithelial cell models (Boublil *et al.* 2013; Dergham *et al.* 2012, 2015; Longhin *et al.* 2013, 2016; Zhou *et al.* 2014). Other studies supported that organic extractable matter (OEM) prepared from PM can contain a mixture of carcinogenic and/or toxic compounds; they evaluated its roles in the overall toxicity but failed to clearly decipher the underlying mechanisms (Akhtar *et al.* 2010; Alessandria *et al.* 2014; De Brito *et al.* 2013, Healey *et al.* 2006, Oh *et al.* 2011, Xiang *et al.* 2018).

In view of the literature supporting the critical role of the organic chemical fraction of airborne PM in its harmful effects on human health, further toxicological researches are requested to gain more knowledge about the crucial role played by the organic chemical fraction in the activation of some classical underlying mechanisms of toxicity. The objectives of this pilot work were also to better investigate the toxicological effects of OEM prepared from $PM_{2.5}$ collected in Beirut (Lebanon), in an urban surrounding, on normal human bronchial epithelial cells (BEAS-2B). After having chemically characterized this OEM, we sought to better investigate some underlying mechanisms possibly involved in its cellular and molecular toxicological effects, with regards to specific endpoints of cytotoxicity, oxidative stress, inflammation, metabolic activation, genotoxicity, and cell cycle deregulation.

2 - MATERIALS AND METHODS

2.1. Chemicals

All the cell culture reagents, the Vybrant Cytotoxicity Assay Kit, the FxCycle PI/RNase Staining Solution, the High Capacity cDNA Reverse Transcription Kit, the Taqman fast advanced Master Mix, Taqman gene expression assays, and the Pierce™ BCA Protein Assay Kit were provided by Thermo-Fisher scientific (Villebon-sur-Yvette-France). CellTiter-Glo® Luminescent Cell Viability was from Promega (Charbonniere-les-Bains, France). Benzo[*a*]Pyrene (B[*a*]P), superoxide dismutase (SOD) determination kit, and other chemical regents were from Sigma Aldrich (France). AllPrep DNA/RNA/miRNA Universal Kit was from QIAGEN (Beirut - Lebanon). TransAM® NRF2 was from Active Motif (La Hulpe, Belgium). 8-isoprostane (8-Isop) ELISA kit was from Abcam (Paris, France). Highly-sensitive 8-hydroxy-2'-deoxyguanosine (8-OHdG) Check was from Gentaur France SARL (Paris, France). MILLIPLEX® MAP Human Cytokine/Chemokine Magnetic Bead Panel- Immunology Multiplex Assay, MILLIPLEX® map 7-plex DNA Damage/Genotoxicity Kit, and the 7-Plex Early Apoptosis Magnetic Bead Kit 96-well Plate Assay were from Merck-Millipore (St Quentin-en-Yvelines, France).

2.2. Sampling site description

Air derived-PM samples were collected in the old airport avenue situated in south Beirut suburb (33° 50′ 59″ N; 35° 29′ 57″ E) from the 9th of November 2015 to the 28th of January 2016 (See supplemental material: Figure S1-A, B, and C). The sampling site was placed close to one of the busiest area of the city, characterized by huge road traffic, large residential areas, the proximity of three important hospitals, and several commercial centers. About at 2 km from the study site is located the Rafic Hariri International airport, characterized by an important aerial traffic. Beirut is characterized by a high transport density and this sector is known to be one of the main causes of air pollution in Lebanon, due to the absence of organized public transport resulting in the duplication, each year, of the number of private cars, mainly gasoline engines. Moreover, Beirut suffers from a major problem that relies on the use of private electric generators diesel powered, in order to fill the gap of the shortage in electricity production supplied by the public sector. The production of electricity in industrial and residential sectors provided by electric generators diesel powered is estimated to 500 MW (MOEW, 2010). It is also important to note that Lebanon has been subjected to a household waste crisis and wild open burning of waste occurred randomly in Beirut agglomeration during the sampling period.

2.3. Sampling of $PM_{2.5}$

$PM_{2.5}$ was sampled using a high-volume cascade sampler TE-231 single (TISCH®, 40 CFM $PM_{2.5}$ single stage), on a daily basis. The first stage was covered with a slotted glass fiber filter (TISCH, TE-230-WH) to retain particles with aerodynamic diameter higher than 2.5 µm. After this, impaction stage, a Whatman® cellulose-base filter (230 mm x 254 mm) was used as back-up filter to collect PM with aerodynamic diameter smaller than 2.5 µm ($PM_{2.5}$). After each sampling period, filters were dried under laminar flow hood during 48 h and then stored at -20°C until further preparation. At the end of the collection period, 15 filters were selected for both global chemical characterization and toxicological endpoint study. Corresponding wind conditions were mainly from the East

pointing to the East residential areas (See also supplemental material: Figure S1-C). Indeed, wind speed was quite low (<2 $m.s^{-1}$) and would not have favored the dispersion of pollutants during the collection period.

2.4. Chemical characterization of $PM_{2.5}$

PAH quantification was done using gas chromatography-mass spectrometry (GC-MS) after extraction of the pristine filters using dichloromethane as described in section "2.5. Preparation of the OEM". Polychlorodibenzo-p-dioxins (PCDD), polychlorodibenzofurans (PCDF), and polychlorobiphenyls (PCB) were quantified using high resolution/GC-MS, after acid treatment of the pristine filters, followed by soxhlet extraction using toluene, purification on silica and alumina columns, and elution with toluene for PCB quantification, and dichloromethane/hexane mixture for PCDD and PCDF quantification. All the PAH, PCDD, PCDF and PCB quantifications were performed by MicroPollutants Technologie S.A. (Saint Julien les Metz, France). The whole analytical procedure has been already described in details in Borgie *et al.* (2015b) and Cazier *et al.* (2016).

2.5. Preparation of the OEM

Briefly, OEM was prepared from $PM_{2.5}$ using a quarter of each of the 15 filters. Pieces of filters were placed in 3 glass tubes (5 pieces per tube) to which 40 mL of dichloromethane were added before ultrasonic treatment (50 min, 100 W, 20°C). Then, dichloromethane solutions were gathered, filtered using cellulose acetate filters (Sartorius®, 0.45 µm) and slowly evaporated under nitrogen flow to obtain a final volume of 5 mL. Indeed, 1 mL of this dichloromethane solution was dedicated to the organic chemical characterization whereas the remaining 4 mL were totally evaporated under nitrogen flow before being resuspended in 4 mL dimethyl sulfoxyde (DMSO) as described by Borgie *et al.* (2015a). This solution was considered as OEM and used for the toxicological study. Considering the 15 pieces of filters, 212.5 mg of $PM_{2.5}$ were used to extract the organic fraction and the final concentration of the final OEM was 42.5 mg PM-equivalent /mL (PM-eq/mL). This concentration was used to express as µg PM-eq/cm^2 the increasing concentrations of OEM to which BEAS-2B cells were exposed in the toxicological part of this work.

2.6. Toxicity of OEM

2.6.1. Cell culture and exposure

BEAS-2B cells (ATCC® CRL-9609™, ECACC, Wiltshire, UK) were purchased from Sigma-Aldrich (Saint-Quentin Fallavier, France). This cell line, originally derived from normal human bronchial epithelial cells, was obtained from autopsy of non-cancerous individuals. Cell culture methods have already been published elsewhere (Leclercq *et al.* 2017b). Briefly, BEAS-2B cells were cultured in 95% humidified air with 5% CO_2 at 37°C in 75 cm^2 CellBIND® surface plastic flasks (Corning; Sigma-Aldrich) in LHC-9 medium. Before reaching 80% of confluence, cells were subcultured by using 0.25% trypsin/0.53mM versene solution containing 0.5% (w/v) polyvinylpyrrolidone (Sigma-Aldrich). Medium was refreshed every 2-3 days. All the BEAS-2B cells we used derived from the same cell culture. Just before reaching the confluence (<80%), BEAS cells were exposed to control solution (*i.e.*, LHC-9 with DMSO at 0.025% v/v) or OEM (*i.e.*, concentrations ranging from 1 to 30 µg $PM_{2.5}$-eq/cm^2, suspended in LHC-9, with DMSO ≤ 0.025% v/v). After 6, 24 and/or 72 h, aliquots of cell-free culture media were collected and quickly frozen at - 80°C. Cell free-culture supernatants were dedicated to assess cytotoxicity and inflammatory endpoints.

Adherent cells were washed twice with 1mL-aliquots of cold sterile PBS, and either quickly frozen at - 80°C or fixed for flow cytometry analysis. The study of the toxicological endpoints (*i.e.*, cytotoxicity, gene expression, oxidative stress, genotoxicity, apoptosis, and cell cycle) needed the preparation of various cell matrices, as previously described in details by Leclercq *et al.* (2016).

2.6.2. Cytotoxicity

The cytotoxicity of OEM was evaluated after cell exposure to increasing concentrations, ranging from 1 to 30 µg $PM_{2.5}$-eq/$cm^{2,}$ during 6, 24 or 72 h through the determination of intracellular ATP concentration (CellTiter-Glo® Luminescent Cell Viability, Promega) and extracellular G6PD activity (Vybrant Cytotoxicity Assay Kit, Thermo Fisher Scientific). It should be noted that the concentration of DMSO in the cell culture medium did not exceed 0.025% (v/v), which avoided the occurrence of its specific toxicity.

2.6.3. Oxidative stress

Oxidative stress was evaluated firstly by the DNA binding activity of nuclear factor erythroid 2-related factor 2 (NRF2) and the associated gene expression of heme oxygenase 1 (*HMOX)* and NAD(P)H quinone dehydrogenase 1 (*NQO1)*, and secondly by SOD activity, 8-Isoprostane (8-Isop) concentration, and 8-hydroxy-2'-deoxyguanosine (8-OHdG) concentration. NRF2 binding activities were studied using TransAM® NRF2 from Active Motif (Leclercq *et al.* 2018). Gene expressions of *HMOX* and *NQO1* were evaluated using quantitative RT-PCR. Briefly, total RNA were isolated using the RNeasy Mini Kit (Qiagen). After the reverse transcription of 1 µg of total RNA in single-stranded cDNA using the High Capacity cDNA Reverse Transcription Kit, the relative quantitation of the gene expressions was carried out using specific Taqman™ gene expression assays (*HMOX*: Hs0110250_m1, *NQO1*: Hs1045993_g1, ARN18S: Hs99999901_s1), a StepOnePlus™ Real-Time PCR System, and the Expression Suite Software (Thermo Fisher Scientific). The relative change in gene expression was calculated by the ΔΔCT method, normalized against endogenous ribosomal 18S. In other respects, SOD activities were carried out using a commercially available kit (SOD determination kit, Sigma-Aldrich) as described elsewhere (Garçon *et al.* 2000). 8-Isop concentrations were determined using 8-isoprostane ELISA kit from Abcam (Leclercq *et al.* 2016). Oxidative DNA adduct 8-OHdG concentrations were studied using a commercially available enzyme immunoassay (Highly Sensitive 8-OHdG Check, Gentaur France SARL), as published elsewhere (Leclercq *et al.* 2016).

2.6.4. Inflammation

Several inflammatory cytokines (tumor necrosis factor, TNF-α; interleukin-1 beta, IL-1β, interleukin-6, IL-6; interleukin-8, IL-8; monocyte chemoattractant protein-1, MCP-1; interferon-gamma, IFN-γ) were determined in cell-free culture supernatants using a MILLIPLEX® MAP Human Cytokine/Chemokine Magnetic Bead Panel-Immunology Multiplex Assay (Merck-Millipore) according to the manufacturer's instructions.

2.6.5. Xenobiotic-metabolizing enzyme gene expression

Expressions of some of the genes closely involved in the AhR signaling pathway and, therefore, in the metabolic activation of the PAH (*i.e., aryl hydrocarbon receptor, AHR; aryl hydrocarbon receptor nuclear translocator, ARNT; cytochrome P450 1A1, CYP1A1; cytochrome P450 1B1, CYP1B1*) were evaluated using

quantitative RT-PCR, as above-described, using specific Taqman™ gene expression assays (*AHR*: Hs00169233_m1, *ARNT*: Hs01121918_m1, *CYP1A1*: Hs01054797_m1, *CYP1B1*: Hs00164383_m1, *ARN18S*: Hs99999901_s1).

2.6.6. Cell cycle

Just after their exposure, BEAS-2B cells were washed twice with DPBS, carefully fixed in 70% (v/v) ethanol, washed again twice with DPBS, and thereafter resuspended in FxCycle PI/RNase stain for 30 min at room temperature. The FxCycle™ PI/RNase Staining Solution, provided as ready-to-use by Thermo-Fisher scientific, was formulated with DNase-free RNase A and a permeabilization reagent in DPBS. Propidium iodide (PI) bind to DNA by intercalating between the bases with little or no sequence preference and with a stoichiometry of one dye per 4-5 base pairs of DNA. Once the dye has been bound to nucleic acids, its fluorescence was analyzed using 488 nm excitation, and a 585/42 nm bandpass filter emission by flow cytometry (Attune® Acoustic Focusing Cytometer; Life Technologies, France). The flow cytometric analysis of the stained cell populations was then used to produce a frequency histogram that reveals the proportion of the cells in each of the different phases of the cell cycle (Attune™ NxT Flow Cytometer Software).

2.6.7. Genotoxicity and apoptosis

Genotoxicity and apoptosis were respectively evaluated using the MILLIPLEX® map 7-plex DNA Damage/Genotoxicity Kit (phosphorylated checkpoint kinase 1, pChk1 (Ser345); phosphorylated checkpoint kinase 2, pChk2 (Thr68); phosphorylated H2A histone family member X, γH2AX (Ser139); phosphorylated protein 53, pP53 (Ser15); total serine/threonine protein kinase, ATR; total mouse double minute 2 homolog, MDM2; and total protein 21, p21), and the 7-Plex Early Apoptosis Magnetic Bead Kit (phosphorylated AKT/protein kinase B, pAKT/PBK (Ser473); phosphorylated c-Jun N-terminal kinase/Serine/threonine-protein kinase, pJNK/SAPK1 (Thr183/Tyr185); phosphorylated BCL-2-associated death promoter, pBAD (Ser112); phosphorylated B-cell lymphoma 2, pBCL-2 (Ser70); phosphorylated protein 53, pP53 (Ser46); active Caspase-8 (Asp384) and active Caspase-9 (Asp315)), according to the manufacturer's recommendations (Merck-Millipore). After their exposure to EOM, BEAS-2B cells were collected and centrifuged (10,000 g for 10 min at 4°C), before the preparation of protein extracts. Protein concentrations were determined by bicinchoninic acid assay (Pierce™ BCA Protein Assay Kit, Thermo Fischer Scientific) before the dilution of the samples to a concentration of 20 µg/well. Analyses were then led scrupulously following the manufacturer's instructions.

2.6.8. Statistical analysis

Results are expressed as mean values and standard deviations. For each incubation time, results from BEAS-2B cells exposed to OEM at its different $PM_{2.5}$-eq concentrations or B[*a*]P were compared to those obtained from non-exposed cells. Statistical analyses were performed by the non-parametric Mann-Whitney U-test with correction for multiple comparisons (Software: SPSS for windows). Significant differences were reported with p values < 0.05.

3. RESULTS

3.1. Chemical characteristics of $PM_{2.5}$

The mean concentration of $PM_{2.5}$ was calculated by considering the total mass of particles collected on each filter during the whole sampling period and the total volume of filtered air. This concentration was estimated at 48 µg/m^3. The 16 PAHs listed by the US-EPA were quantified and their concentrations are given in Table 1. The total PAH concentration was 9.7 ng/m^3. Benzo[*b*]fluoranthene (B[*b*]F), chrysene (CHR), benz[*a*]anthracene (B[*a*]A), pyrene (PYR) and benzo[*ghi*]perylene (B[*ghi*]P) were the most abundant with values between 989 and 1519 pg/m^3 (or 20.6 and 31.6 µg/g $PM_{2.5}$). Moreover, there were several polychlorinated highly persistent compounds such as PCDD, PCDF and DL-PCB within the sampled particles. Indeed, total concentrations of PCDD, PCDF and PCB were about 459 fg/m^3 (or 9,587 pg/g $PM_{2.5}$), 560 fg/m^3 (or 12,255 pg/g $PM_{2.5}$), and 949 fg/m^3 (or 19,818 pg/g $PM_{2.5}$) respectively, as shown by Table 2. According to the respective toxicity of the congeners, as defined by Van den Berg *et al.* (2005), their total concentration, as expressed by international toxic equivalent quantity (I-TEQ) was about 58 fg I-TEQ/m^3 (or 1,217 pg I-TEQ/g).

3.2. Cytotoxicity of OEM

As shown in Figure 1, significant decreases of ATP levels were observed in BEAS-2B cells 72 h after their exposure to increasing concentrations ranging from 5 to 30 µg $PM_{2.5}$-eq/cm^2 *versus* control ($p < 0.05$). Concerning G6PD activity, significant increases were seen in BEAS-2B cells only 72 h after their exposure to OEM at 15 and 30 µg $PM_{2.5}$-eq/cm^2 *versus* control ($p < 0.01$).

3.3. Oxidative effects of OEM

Figure 2 showed the dose-dependent increases of NRF-2 binding activity observed in BEAS-2B cells 6 h after their exposure to [OEM] eq $PM_{2.5}$ at 15 and 30 µg/cm^2, and to B[*a*]P, and 24 h after their exposure to [OEM] eq $PM_{2.5}$ at 3, 15 and/or 30 µg/cm^2, and to B[*a*]P *versus* control ($p < 0.05$). Significant inductions of both *HMOX* and *NQO1* gene transcription were reported in BEAS-2B cells, 6 h after their exposure to OEM at 3, 15 and/or 30 µg $PM_{2.5}$-eq/cm^2, and to B[*a*]P ($p < 0.05$), and 24 h after their exposure to OEM at all the tested concentrations, and to B[*a*]P ($p < 0.05$). With regards to SOD activity, statistically significant increases were observed in BEAS-2B cells 6 h after their exposure to OEM at 30 µg $PM_{2.5}$-eq/cm^2,and to B[*a*]P, and 24 h after their exposure to OEM at 15 and 30 µg $PM_{2.5}$-eq/cm^2, and to B[*a*]P *versus* control ($p < 0.05$). Whatever the incubation times and exposure conditions, significant increases of 8-Isop concentrations were reported in BEAS-2B cells ($p < 0.05$). Moreover, dose-dependent increases of 8-OHdG were seen in BEAS-2B cells 6 h and 24 h after their exposure to OEM and to B[*a*]P *versus* control ($p < 0.05$).

3.4. Inflammatory effects of OEM

As shown in Figure 3, no statistically significant change of the secretion of all the cytokines under study (TNF-α, IL-1β, IL-6, IL-8, MCP-1, IFN-γ) was reported in EOM-exposed BEAS-2B cells, whatever the exposure

conditions and incubation times. A significant increase of the concentration of IFN-γ was observed in the supernatants of BEAS-2B cells 24 h after their exposure to B[a]P *versus* control ($p < 0.05$).

3.5. Xenobiotic-metabolizing enzyme gene induction by OEM

Whatever the incubation times and the exposure conditions, no statistically significant change of *AHR* and *ARNT* gene expression was observed in BEAS-2B cells (Figure 4). In contrast, a statistically significant induction of *CYP1A1* and *CYP1B1* gene transcription was reported in BEAS-2B cells whatever the incubation times (6 and 24 h) and exposure conditions (3, 15 and 30 μg $PM_{2.5}$-eq/cm^2, or to B[*a*]P) *versus* control ($p < 0.05$).

3.6. Genotoxic effects of OEM

Figure 5 showed slight but statistically significant increases of phosphorylated-P53 (pP53) concentrations in BEAS-2B cells 72 h after their exposure to increasing concentrations of OEM, and to B[*a*]P *versus* control ($p < 0.05$). With regards to P21 concentrations, significant increases was reported only in BEAS-2B cells 6 h after their exposure to B[*a*]P *versus* control ($p < 0.05$). Whatever the incubation times and exposure conditions, slight but significant decreases of phosphorylated-H2AX (γH2AX) concentrations, most often statistically significant, were reported in BEAS-2B cells ($p < 0.05$). In contrast, no significant change of total MDM-2 concentrations was observed. There were slight but significant increases of phosphorylated-CHK-1 (pCHK-1) concentrations in BEAS-2B cells 72 h after their exposure to OEM from 3 to 30 μg $PM_{2.5}$-eq/cm^2 *versus* control ($p < 0.05$). Similarly, slight but significant increases of phosphorylated CHK-2 (pCHK-2) concentrations were observed in BEAS-2B cells 72 h after their exposure to OEM at the two highest concentrations, and to B[*a*]P *versus* control ($p < 0.05$).

3.6. Cell cycle effects of OEM.

As shown in Figure 6, most of control and exposed BEAS-2B cells were in the S phase after 24 h: from 40.07 ± 4.57 % for the control cells to 49.48 ± 4.75 % for 15 μg $PM_{2.5}$-eq/cm^2 exposed cells. Indeed, there were slight increases of the percentages of BEAS-2B cells in the S phase in BEAS-2B cells 24 after their exposure to OEM, particularly at the two highest concentrations (49.48 ± 4.75 % for 15 μg $PM_{2.5}$-eq/cm^2 and 48.53 ± 0.75 % for 30 μg $PM_{2.5}$-eq/cm^2), *versus* control (40.07 ± 4.57 %). In contrast, the majority of control and exposed BEAS-2B cells were in the G1 or S phases after 72 h. There were also slight increases of the percentages of BEAS-2B cells in the G1 phase 72 h after their exposure to OEM at the highest concentration (29.39 ± 2.93 % for 30 μg $PM_{2.5}$-eq/cm^2) and B[a]P (28.71 ± 2.74 %), *versus* control (23.25 ± 2.45 %). Moreover, very slight increases of the percentages of BEAS-2B cells in the S phase were reported 72 h after their exposure to OEM at the different concentrations (30.98 ± 0.95 % for 3 μg $PM_{2.5}$-eq/cm^2 and 30.00 ± 0.71 % for 30 μg $PM_{2.5}$-eq/cm^2), *versus* control (28.97 ± 0.47 %).

3.7. Apoptotic effects of OEM.

Generally relatively low but statistically significant increases in phosphorylated-AKT (pAKT) concentrations were observed in BEAS-2B cells 24 and 72 h after their exposure to OEM at the two highest concentrations, and to B[*a*]P *versus* control ($p < 0.05$) (Figure 7). However, no significant phosphorylation of JNK was detected in BEAS-2B cells after their exposure to OEM nor to B[*a*]P. In contrast, for all the incubation times and exposure conditions to EOM, slight but significant increases of phosphorylated-BAD (pBAD) concentrations but not phosphorylated-

BCL-2 (pBCL-2) concentrations were reported in BEAS-2B cells *versus* control ($p<0.05$). Only a 72 h incubation of the BEAS-2B cells with B[a]P lead to a statistically significant increase of pBAD concentrations *versus* control ($p<0.05$). The active forms of caspase-8 and -9 were not statistically modified in BEAS-2B cells 24 h nor 72 h after their exposure to each of the tested conditions.

4. DISCUSSION

Despite the high number of *in vitro* approaches reported in the respiratory toxicology literature, researchers are still far from having a complete detailed mechanistic explanation of the causal relation between PM and health effects (Longhin *et al.* 2016). There is still a lack of knowledge about the specific chemical fraction within particles, which could be mainly responsible of its adverse effects on human health. Hence, this work aimed to better decipher the toxicological effects of the OEM from ambient $PM_{2.5}$ on normal human bronchial epithelial cells (BEAS-2B).

Fine particles were collected close to one of the busiest area in the southern suburb of Beirut (Lebanon). Their average concentration (48 µg/m^3), 1.9 times higher than the daily $PM_{2.5}$ World Human Organization guideline (25 µg/m^3), was in line with those recently reported in Beirut (41 µg/m^3) by Borgie *et al.* (2015a) but also higher than others observed few years ago in Beirut (20 µg/m^3) by Massoud *et al.* (2011), and in the suburb (28 µg/m^3) by Saliba *et al.* (2010). The mean total concentration of PAH (9.7 ng/m^3) found in these particles was higher (8.3 and 28-times, respectively) than those reported in 2011 in the Sin El Fil district of Beirut (1.16 ng/m^3) and in Bejje (0.35 ng/m^3), a rural area located in the north of Lebanon. Benzo[*b*]fluoranthene (B[*b*]F), the most abundant congener, generally reflects the contribution of diesel power generator and diesel trucks and buses as personal cars only runs with gasoline. The fleet of vehicles in Beirut is generally old and use low quality fuel oil, which is problematic considering the daily density of traffic. Chrysene (CHR), the second most abundant congener, is often generated during oil distillation process or waste incineration (Borgie *et al.* 2015a). To better determine the sources of PAH, ratios were calculated referring to Ravindra *et al.* (2008) (Table 3). Diesel exhaust was also incriminated as a PAH contributing source with ratios of indeno[*1,2,3-cd*]pyrene (I[*cd*]P)/(I[*cd*]P + benzo[*ghi*]perylene (B[*ghi*]P)) = 0.33 and Benzo[*a*]pyrene (B[*a*]P)/(B[*a*]P + Chrysene (CHR)) = 0.3. These emissions could be related to the use of generators, to compensate the lack of electricity provided by the Lebanese state. In addition, vehicular emissions and the use of gasoline engines were evidenced by Fluoranthene (FLT)/Pyrene (PYR) = 0.6 and PYR/B[*a*]P = 2, which were in agreement with the huge road traffic occurring in Beirut. Reported levels of PCDD (449 fg/m^3) and PCDF (560 fg/m^3) were higher (2.1 and 6.5 times, respectively) than those obtained in 2011 in the Sin El Fil district of Beirut (214 and 87 fg/m^3, respectively) (Borgie *et al.* 2015a). The high concentrations of dioxins and furans we found could be correlated with the recent worrying problem of waste occurring in Lebanon since July 2015, resulting in uncontrolled open waste burning. Indeed, in 2016, Baalbaki *et al.* found PCDD and PCDF levels near an open-air waste burning site in Beirut higher (2.2 and 16,4-fold, respectively) than those above-reported. Taken together, these data supported that the $PM_{2.5}$ samples collected in this work contained a wide variety of chemicals including PAH and other related-chemical compounds (*e.g.*, PCDD, PCDF, DL-PCB).

This work was carried out on normal human bronchial epithelial BEAS-2B cells, a dedicated cell model, mainly due to its relatively high homology to human lung tissues and primary cells (Courcot *et al.* 2012). In BEAS-2B cells, the dose- and time-dependent cytotoxicity induced by OEM was used to choice the concentrations (from 1 to 30 µg $PM_{2.5}$-eq/cm²) and the kinetic (from 6 to 72 h) to apply for the further study of the other toxicological endpoints.

PAH and other related-chemical compounds found in the $PM_{2.5}$ samples under study have been rather associated with early oxidative events and inflammation in human bronchial epithelial cell models (Boublil *et al.* 2013; Dergham *et al.* 2012, 2015; Gualtieri *et al.* 2010, 2011; Longhin *et al.* 2013, 2016; Zhou *et al.* 2014). Because of its key role as master regulator of the cell redox homeostasis, NRF-2 is well-equipped to counteract the cytosolic

ROS production and is critical for maintaining the redox balance in the cell (Wardyn *et al.* 2015). Following exposure to oxidants or electrophiles, NRF2 accumulates in the nucleus where it binds to antioxidant response element in the upstream regulatory regions of genes encoding NRF-2 targets including antioxidant enzymes, proteins involved in xenobiotic metabolism and clearance, protection against metal toxicity, inhibition of inflammation, repair and removal of damaged proteins, as well as other transcription and growth factors (Suzuki *et al.* 2016). In this work, dose- and time-dependent significant increases of NRF-2 binding activity and NRF-2 target gene transcription (*i.e.*, *HMOX1* and *NQO1*) or target protein (*i.e.*, SOD) were seen in OEM-exposed BEAS-2B cells. Indeed, some transcription factors, such as NRF2, can be activated by electrophilic metabolites arising through the metabolic activation of PAH (Nguyen *et al.* 2009; Lawal, 2017). Despite the clear activation of the NRF-2 signaling pathway, somewhat surprisingly, there were anyway dose- and time-dependent significant lipid peroxidation and oxidative DNA adduct formation. Indeed, 8-isoP is a lipid peroxidation product of arachidonic acid which has been identified as one of the most useful biomarkers of oxidative damage (Erve *et al.* 2017). In DNA, 8-OHdG is considered as one of the predominant forms of ROS-induced oxidative lesions and has also been widely used as a biomarker for oxidative stress (Valavanidis *et al.* 2009). Taken together, these data closely supported that OEM actively contributed to redox imbalance, thereby activating the NRF-2 signaling pathway; however, for the most harmful conditions, chemical-catalyzed ROS overproduction, notably through the metabolic activation of organic chemicals, was not totally counteracted, thereby leading to oxidative damage to some critical macromolecules (Boublil *et al.*, 2013; Dergham *et al.*, 2012, 2015; Leclercq *et al.* 2018; Longhin *et al.* 2013; Zhou *et al.*, 2014).

While NRF-2 is an anti-inflammatory, the inhibition of the inflammation by NRF-2 is generally associated with the inhibition of the NF-κB signaling pathway and, therefore, that of the inflammatory cytokine production (Fischer *et al.* 2015; Ma *et al.* 2013). According to the above-reported activation of the NRF-2 signaling pathway, OEM exposure did not trigger any significant change in the secretion of inflammatory cytokines (*i.e.*, TNFα, IL-1β, IL-6, IL-8, MCP-1, and IFNγ). However, the proinflammatory properties of various types of air pollution-derived PM have already been largely described (Boulbil *et al.* 2013; Ghio *et al.* 2013; Gualtieri *et al.* 2010, 2011; Leclercq *et al.* 2016, 2017a, 2017b, 2018; Longhin *et al.* 2013; Loxham *et al.* 2015). There seemed also to be a striking disconnect between the proinflammatory properties of whole PM, on the one hand, and of OEM, on the other hand. This apparent discrepancy could possibly relies on the specific roles played by particles themselves, as carrier of various coated-organic chemicals, in the efficient absorption of these organic chemicals by epithelial cells and/or in the induction of some of the underlying mechanisms clearly related to the initiation and/or exacerbation of the inflammatory response (*e.g.*, endocytosis mechanisms) (Garçon *et al.*, 2000, 2004; Gosset *et al.*, 2003).

In general, metabolic activation is beneficial in helping lung cells to reduce the potential toxicity of inhaled pollutants. However, sometimes, it transforms harmless substances into electrophile metabolites that are highly reactive towards endogenous macromolecules, thereby producing toxicity (Saint-Georges et *al.* 2008, 2009). In this work, CYP1A1 and 1B1 isoforms, constitutively poorly or not expressed in bronchial tissues, exhibited high transcription levels in BEAS-2B cells already 6 h until 24 h after their exposure to OEM, enriched in PAH, PCDD, PCDF, and PCB. Gualtieri *et al.* (2011) reported that, due to their relatively high contents of PAH, PM_{10} and $PM_{2.5,}$ representative of background urban air pollution, diesel exhaust particles, and wood smoke were all able to significantly activate the AHR signaling pathway in BEAS-2B cells. Oh *et al.* (2011) indicated that OEM which contain aliphatic chlorinated hydrocarbons, PAH/their alkyl derivatives, and nitro-AH/ketones/quinones, induced

CYP1A1-dependent EROD activity, through AHR signaling pathway activation, which is specifically related to the critical role of the organic chemical fraction of ambient PM.

Despite the alkyl and oxidative DNA adducts generally reported in human bronchial epithelial cells exposed to whole PM or OEM, significant changes in primary DNA single-strand breaks (SSB), DNA double-strand break (DSB), and chromosomal aberrations were not systematically reported (Andre *et al.* 2011, Borgie *et al.* 2015b, Leclercq *et al.* 2017a, Lepers *et al.* 2014, Oh *et al.* 2011). There is now overwhelming evidence that ambient air contains hundreds of genotoxic compounds; however, some apparent difference in the genotoxic potential might probably rely on the use of different materials, cell models, and exposure strategies. There is also still an urgent need to better investigate the genotoxic potential of OEM. It was reported several years ago, that in mammalian cells the phosphorylation of the subtype of histone H2A, called H2AX, in the position of Ser139 occurs in response to DSB formation (Podhorecka *et al.* 2010). Due to the fact that *γ*H2AX appears early and forms foci at damage sites, it is widely considered to be a ensitive biomarker for DSB (Tu *et al.* 2013). However, in this work, OEM induced slight but significant decreases of H2AX phosphorylation, thereby indicating an important default in the repair of genetic material. Bouquet *et al.* (2006) reported that γH2AX loss correlates with DSB repair activity only at low cytotoxic doses, when less than 100-150 DSB breaks per genome are produced, independently of the method used. Their results suggested that the dephosphorylation step of γH2AX may be limiting and that the loss of foci is mediated not only by γH2AX dephosphorylation but also through its redistribution towards the chromatin. Since the phosphorylation of H2AX is linearly related to the dose used, although dependent on the cell line, the phosphatase activity might represent the limiting step leading to a persistent signal. Finally, it is conceivable that the γH2AX might also be targeted for degradation, a step that might be saturable, as observed in this work. The γH2AX decreases also reported within BEAS-2B cells after their exposure to low cytotoxic doses of OEM can therefore be related to the higher levels of phosphorylated P53, CHK-1 and CHK-2 proteins, generally closely associated with cell cycle arrest (Fragkos *et al.* 2009). The tumor suppressor protein P53 plays a critical role in cell fate determination. Especially after DNA damage, P53 plays an anti-apoptotic role through activation of P21, which induces cell cycle arrest, and facilitates DNA repair. However, when DNA damage exceeds a threshold or is so severe that it cannot be repaired, P53 promotes apoptosis (Shin *et al.* 2015). It might be expected that the OEM-induced P53 phosphorylation reported in this work, concurrent with DNA damage, would lead to cell cycle arrest, as reported by Gualtieri *et al.* (2011). These authors indicated that BEAS-2B cell exposure to whole $PM_{2.5}$ resulted in DNA damage, giving DNA-damage response characterized by increased phosphorylation of ATM and CHK2, but, contrary to the present results, increased phosphorylation of γH2AX, with an apparent lack of G2-arrest.

To go further in this work, the cell cycle was analyzed. After 24 h, the cell cycle profile of control cells clearly indicated that they were already stalled in S-phase. There were also slight increases of the percentages of BEAS-2B cells in the S phase after their exposure to OEM, particularly at the two highest concentrations. In contrast, after 72 h, the cell cycle profile of control cells showed that the majority of cells were in G1 and S phases. There were also only very slight increases of the percentages of BEAS-2B cells in both these phases 72 h after their exposure to OEM. The response to DNA damage, as those previously reported through the excessive 8-OHdG formation in OEM-exposed BEAS-2B cells, is an inherent part of the cell cycle and its main action is to halt cell cycle progression and establish a checkpoint (G1/S, intra-S, G2/M, and M). At these positions a cell can stop or slow down in case of unfavorable conditions, stress or DNA damage. Chen *et al.* (2016) also reported that different sizes and shapes of

TiO_2 nanomaterials (AFDC and cNRs) could inhibit the growth of BEAS-2B cells and allow a considerable proportion of them to remain in the G1/G0 phase: in the low-concentration exposure, the cell cycle was terminated during the G1/G0 phase without apparent cell death, whereas in the high-concentration exposure, the dramatic decrease in cell viability was contributed by apoptotic cell death. To take care of DNA damage, repair mechanisms are put in place and if possible, a cell eventually continues proliferation or exits the cell cycle (Bertoli *et al.* 2013; Iyer *et al.* 2017). In particular, cells activate the intra-S checkpoint in response to damage during S phase to protect genomic integrity and ensure replication fidelity. Accordingly, in this work, most of the OEM-exposed BEAS-2B cells were in the S phase after 24 h. The checkpoint prevents genomic instability mainly by regulating origin firing, fork progression, and transcription of G1/S genes in response to DNA damage. Despite having specific repair pathways dedicated to each kind of DNA lesion, the cell relies on a single checkpoint to mediate the DNA damage response during S phase. The cell has two main checkpoint kinases, Rad3-related (ATR) and ataxia telangiectasia mutated (ATM), both of which are critical for maintaining genomic integrity. ATR and ATM activate two effector kinases, CHK1 and CHK2, in response to damage to relay the checkpoint signal across the cell. Accordingly, in this work, there were slight but significant increases of phosphorylated-CHK-1 and/or CHK-2 concentrations in BEAS-2B cells 72 h after their exposure to OEM. Although CHK1 is primarily activated by ATR in response to various kinds of lesions and CHK2 by ATM in response to DSB, there is substantial cross-talk between the two pathways making it difficult to unambiguously assign CHK1 and CHK2 to a single checkpoint pathway (Iyer *et al.* 2017). Relatively low but statistically significant increases in the phosphorylation of AKT were observed in BEAS-2B cells 24 and 72 h after their exposure to OEM at the two highest concentrations. Zhang et al. (2013) investigated the role of CYP2A13, an extrahepatic enzyme that mainly expresses in human respiratory system, in the metabolic activation of aflatoxin G1, in BEAS-2B cells that stably express CYP2A13 (B-2A13). They reported that low concentrations of aflatoxin G1 induced S phase arrest and DNA damage in B-2A13 cells, and the proteins related to DNA damage responses, such as ATM, ATR, Chk2, p53, BRCA1, and cH2AX, were activated. For all the incubation times and exposure conditions we tested, slight but significant increases of phosphorylated-BAD concentrations were reported in BEAS-2B cells. Taken together, these results clearly indicated the survival of the exposed cells with possible blockages of their cell cycle in G1/S and intra-S checkpoints. In response to replication stress, CHK1, reported as slightly but significantly phosphorylated in BEAS-2B cells 72 h after their exposure to OEM, could be responsible for inactivating G1-S transcription (Bertoli *et al*. 2013). This transcriptional response seems to be specific for replication stress, which, in contrast to the DNA damage response, does not induce apoptosis, according to the results of the present work. Accordingly, there were also slight increases of the percentages of BEAS-2B cells in the G1 phase 72 h after their exposure to OEM. Gualtieri *et al.* (2011) reported that, in accordance with the observed DNA damage, whole $PM_{2.5}$ also induced activation of the ATM/CHK2 pathway in BEAS-2B cells, without any apparent arrest of cells in G2 suggesting that the G2/M checkpoint failed. In contrast, they did not observe any increase in the activation of the ATR/CHK1 pathway, which would be expected following DNA DSB and stalled DNA replication. Wu *et al.* (2017) hypothesized that exposure to whole PM could trigger cell cycle arrest in G2/M phase and DNA damage in BEAS-2B cells, thereby activating the expression of related proteins. According to these results, Zhuang *et al.* (2011) reported increases of the levels of phosphorylated AKT, which plays an important role in survival pathways by inactivating downstream pro-apoptotic factors in many cell systems. According to the results reported in the present work, ROS-activated AKT could participate in ultrafine carbon black-induced cell proliferation, and

mediates pro-carcinogenic effects induced by diesel exhaust particle and smoking compounds, respectively (Park *et al.* 2013, Weissenberg *et al.* 2010). Moreover, Zhou et al. (2016) observed continuous elevation of ROS and concomitant phospho-activation of AKT in BEAS-2B cells during exposure to whole $PM_{2.5}$. These changes were blocked by pretreatment with the free-radical scavenger NAC, suggesting that $PM_{2.5}$ activates AKT by increasing ROS; this latest result was closely related to our own observations supporting that OEM induced a noticeable oxidative stress. Furthermore, in this work, for all the incubation times and exposure conditions, slight but significant increases of phosphorylated-BAD concentrations were reported. According to Datta et al. (1997), AKT phosphorylates BAD *in vitro* and *in vivo*, and may thereby suppress BAD-induced cell death and promote cell survival. It is also noteworthy that, in this work, both caspase 8 and 9 activities were not significantly changed in BEAS-2B-exposed to OEM, thereby supporting the absence of clear apoptotic events. In contrast, Abbas *et al.* (2010, 2016), studying the sequential occurrence of molecular abnormalities from TP53-RB gene signaling pathway activation in the L132 target human lung epithelial cell model, reported that relatively high doses of $PM_{2.5}$ altered the gene expression and/or the protein concentration of several key cell cycle controllers from TP53-RB gene signaling pathway, thereby leading to the occurrence of cell proliferation and apoptosis together. Taken together, these results might ask the critical question whether there is a balance or, in contrast, there will rather be an imbalance between the cell survival, cell proliferation and cell death possibly occurring in whole PM or OEM-exposed cells, depending of the dose applied. However, the results reported in this work, despite the fact that only the active forms of the different key endpoints were studied without correction to their respective total forms, clearly indicated that exposure to EOM induced cell deregulation through blockages of their cell cycle in G1/S and intra-S checkpoints, and even cell survival.

5. CONCLUSION

In this work, we demonstrated that the OEM derived from ambient $PM_{2.5}$ collected in urban surroundings was enriched in PAH and other related chemical compounds, which could also trigger some underlying mechanisms of toxicity, and a combination thereof may be same or different compared with those induced by whole PM. Indeed, acute exposure to OEM at relatively low concentrations activated the AHR and NRF2 signaling pathways but, contrary to whole PM, failed to trigger an inflammatory response. Moreover, these results closely supported the capacity of EOM to trigger cell deregulation notably through blockages of their cell cycle in G1/S and intra-S checkpoints, and even cell survival. In view of the original data reported in this preliminary work, future complementary works are also needed to better decipher the critical role of OEM on the cell cycle regulation. In these future complementary works, it could be more insightful to investigate the toxicity of OEM together with those of whole $PM_{2.5}$, to which it has been extracted, and with non-organic fraction (*i.e.*, residual $PM_{2.5}$ after OEM extraction), to allow to compare the adverse effects from the OEM fraction with both total and residual $PM_{2.5}$ fractions.

ACKNOWLEDGMENTS

The research described in this article benefited from grants from the National Council for Scientific Research of Lebanon (Grant Research Program, Ref: 04-06-2014). The “Unité de Chimie Environnementale et Interactions sur le Vivant” (UCEIV-EA4492) and the “IMPacts de l’Environnement Chimique sur la Santé Humaine” (IMPECS-EA4483) both participate in the CLIMIBIO project, which is financially supported by the Hauts-de-France Region Council, the French Ministry of Higher Education and Research, and the European Regional Development Funds.” The authors would like to thank Dr A. HACHIMI from Micropolluants Technologie, for the determination of PAH and other related chemicals within air pollution-derived $PM_{2.5}$.

REFERENCES

AQiE, A. Q. (2016). Technical report, Copenhagen.

Abbas, I., Saint-Georges, F., Billet, S., Verdin, A., Mulliez, P., Shirali, P., & Garçon, G. (2009). Air pollution particulate matter ($PM_{2.5}$)-induced gene expression of volatile organic compound and/or polycyclic aromatic hydrocarbon-metabolizing enzymes in an in vitro coculture lung model. *Toxicol. in Vitro 23*(1), 37-46.

Abbas, I., Garçon, G. Saint.-Georges, F., Billet, S., Verdin, A., Gosset, P., Shirali, P. (2010). Occurrence of molecular abnormalities of cell cycle in L132 cells after in vitro short-term exposure to air pollution $PM_{2.5}$. *Chem. Biol. Interaction 88*(3), 558-565.

Abbas, I., Verdin, A., Escande, F., Saint-Georges, F., Cazier, F., Mulliez, P., Garçon, G. (2016). In vitro short-term exposure to air pollution $PM_{2.5-0.3}$ induced cell cycle alterations and genetic instability in a human lung cell co-culture model. *Environ. Res. 147*, 146-158.

Abbas, I., Badran, G., Verdin, A., Ledoux, F., Roumié, M., Courcot, D., Garçon, G. (2018). Polycyclic aromatic hydrocarbon derivatives in airborne particulate matter: sources, analysis and toxicity. *Environ. Chem. Lett.* 16 (2), 439-475.

Akhtar, U. S., Mcwhinney, R. D., Rastogi, N., Abbatt, J. P., Evans, G. J., Scott, J. A. (2010). Cytotoxic and proinflammatory effects of ambient and source-related particulate matter (PM) in relation to the production of reactive oxygen species (ROS) and cytokine adsorption by particles. *Inhal. Toxicol. 22*, 37-47.

Alessandria, L., Schiliro, T., Degan, R., Traversi, D., Gilli, G. (2014). Cytotoxic response in human lung epithelial cells and ion characteristics of urban-air particles from Torino, a northern Italian city. *Environ. Sci. Poll. Res., 21* (8), 5554-5564.

Andre, V., Billet, S., Pottier, D., Le Goff, J., Pottier, I., Garçon, G., Shirali, P., Sichel, F. (2011). Mutagenicity and genotoxicity of $PM_{2,5}$ issued from an urbanoindustrialized area of Dunkerque (France). J. Appl. Toxicol. 31 (2), 131-138.

Baalbaki, R., El Hage, R., Nassar, J., Gerard, J., Saliba, N., Zaarour, R., Saliba, N. (2016). Exposure to atmospheric PMS, PAHS, PCDD/FS and metals near an open air waste burning site in Beirut. *Lebanese Sci. J.,* 2, 91-103.

Bertoli, C., Skotheim, J.M. de Bruin, R.A.M. (2013) Control of cell cycle transcription during G1 and S phases. *Nat Rev Mol Cell Biol.* 14 (8), 518-528.

Bouquet, F., Muller, C., Salles, B. (2006). The loss of γH2AX signal is a marker of DNA double strand breaks repair only at low levels of DNA damage. *Cell Cycle* 5 (10), 1116-1122.

Borgie, M., Dagher, Z., Ledoux, F., Verdin, A. C., Martin, P., Courcot, D. (2015 a). Comparison between ultrafine and fine particulate matter collected in Lebanon: Chemical characterization, *in vitro* cytotoxic effects and metabolizing enzymes gene expression in human bronchial epithelial cells. *Environ. Poll. 205*, 250-260.

Borgie, M., Ledoux, F., Verdin, A., Cazier, F., Greige, H., Shirali, P., Dagher, Z. (2015 b). Genotoxic and epigenotoxic effects of fine particulate matter from rural and urban sites in Lebanon on human bronchial epithelial cell. *Environ. Res. 136*, 352-362.

Boublil, L., Assémat, E., Borot, M.C., Boland, S., Martinon, L., Sciare, J., Baeza-Squiban, A. (2013). Development of a repeated exposure protocol of human bronchial epithelium in vitro to study the long-term effects of atmospheric particles. *Toxicol in vitro* 27, 533-542.

Cao, C., Jiang, W., Wang, B., Fang, J., Lang, J., Tian, G., Zhu, T. (2014). Inhalable microorganisms in Beijing's PM2.5 and PM10 pollutants during a severe smog event. *Environ. Sci. Technol.* 48, 1499-1507.

Cazier F., Genevray P., Dewaele D., Nouali H., Verdin A., Ledoux F., Hachimi A., Courcot L., Billet S., Bouhsina S., Shirali P., Garçon G., Courcot D. (2016). Characterisation and seasonal variations of particles in the atmosphere of rural, urban and industrial areas: Organic compounds. J. Environ. Sci., 44, 45-56.

Chen, C., Huang, J-H., Lai, T-C., Jan, Y-H., Hsiao, M., Chen, C-H., Hwuc, Y-K., Liu, R-S. (2016). Evaluation of the intracellular uptake and cytotoxicity effect of TiO^2 nanostructures for various human oral and lung cells under dark conditions. *Toxicol. Res.* 5, 303-311.

Courcot, E., Leclerc, J., Lafitte, J.J., Mensier, E., Jaillard, S., Gosset, P., Shirali, P., Pottier, N., Broly, F., Lo-Guidice, J.M., (2012). Xenobiotic metabolism and disposition in human lung cell models: comparison with in vivo expression profiles. *Drug Metab Dispos.* 40(10): 1953-1965.

Dagher, Z., Garcon, G., Billet, S., Gosset, P., Ledoux F., Courcot, D., Aboukais, A., Shirali, P. (2006). Activation of different pathways of apoptosis by air pollution particulate matter ($PM_{2.5}$) in human epithelial lung cells (L132) in culture. *Toxicology* 225 (1), 12-24.

Datta, S.R., Dudek, H., Tao, X., Masters, S., Fu, H., Gotoh, Y., Greenberg, M.E. (1997). Akt phosphorylation of BAD couples survival signals to the cell-intrinsic death machinery. *Cell* 91, 231-241.

De Brito, K., De Lemos, C., Rocha, J., Mielli, A. C., Matzenbacher , C., Vargas, V. (2013). Comparative genotoxicity of airborne particulate matter ($PM_{2.5}$) using Salmonella, plants and mammalian cells. *Ecotoxicol Environ Saf*., 94, 14-20.

Delfino, R. J., Staimer, N., Tjoa, T., Mohammad, A., Polidori, A., Gillen, D.L., Kleinman, M.T., Schauer, J.J., Sioutas, C. (2010). Association of Biomarkers of Systemic Inflammation with Organic Components and Source Tracers in Quasi-Ultrafine Particles. *Environ. Health Perspect.* 118 (6), 756-762.

Dergham, M., Lepers, C., Verdin, A., Billet, S., Cazier, F., Courcot, D., Garçon, G. (2012). Prooxidant and Proinflammatory Potency of Air Pollution Particulate Matter ($PM_{2.5–0.3}$) Produced in Rural, Urban, or Industrial Surroundings in Human Bronchial Epithelial Cells (BEAS-2B). *Chem. Res. Toxicol*. 5 (4), 904-919.

Dergham, M., Lepers, C., Verdin, A., Cazier, F., Billet, S., Courcot, D., Garçon, G. (2015). Temporal–spatial variations of the physicochemical characteristics of air pollution Particulate Matter ($PM_{2.5–0.3}$) and toxicological effects in human bronchial epithelial cells (BEAS-2B). *Environ. Res.* 137, 256-267.

Erve, T., Kadiiska, M. L., Masona, R. (2017). Classifying oxidative stress by F2-isoprostane levels across human diseases: A meta-analysis. *Redox Biol. 12*, 582-599.

Fragkos, M., Jurvansuu, J., Beard, P. (2009). H2AX is required for cell cycle arrest via the p53/p21 pathway. *Mol. Cell. Biol*. 29 (10), 2828-2840.

Fischer, B.M., Voynow, J.A., Ghio, A.J., (2015). COPD: balancing oxidants and antioxidants, *Int. J COPD* 10, 261-276

Garçon G., Shirali, P. Garry, S., Fontaine, M., Zerimech, F., Martin, A., Hannothiaux, M.H., (2000). Polycyclic aromatic hydrocarbon coated onto Fe_2O_3 particles: assessment of cellular membrane damage and antioxidant system disruption in human epithelial lung cells (L132) in culture. *Toxicol. Lett.* 117 (1-2), 25-35.

Garçon, G., Gosset, P., Zerimech, F., Grave-Descampiaux, B., Shirali, P. (2004). Effect of $Fe_{(2)}O_{(3)}$ on the capacity of benzo(*a*)pyrene to induce polycyclic aromatic hydrocarbon-metabolizing enzymes in the respiratory tract of Sprague-Dawley rats. *Toxicol. Lett.* 150 (2), 179-189.

Ghio, A.J., Dailey, L.A., Soukup, J.M., Stonehuerner, J., Richards, J.H., Devlin, R.B. (2013). Growth of human bronchial epithelial cells at an air-liquid interface alters the response to particle exposure. *Part Fibre Toxicol*, 10, 25.

Gosset, P., Garçon, G., Casset, A., Fleurisse, L., Hannothiaux, M.H., Creusy, C., Shirali, P. (2003). Benzo(a)pyrene-coated onto Fe_2O_3 particles-induced apoptotic events in the lungs of Sprague-Dawley rats. *Toxicol Lett.* 143 (2), 223-232.

Gualtieri, M., Øvrevik, J., Holme, J.A., Perrone, M.G., Bolzacchini, E., Schwarze, P.E., Camatini, M. (2010). Differences in cytotoxicity versus pro-inflammatory potency of different PM fractions in human epithelial lung cells, *Toxicol InVitro* 24, 29-39.

Gualtieri, M., Ovrevik, J., Mollerup, S., Asare, N., Longhin, E., Dahlman, H.J., Camatini, M., Holme, J.A. (2011). Airborne urban particles (Milan winter-$PM_{2.5}$) cause mitotic arrest and cell death: Effects on DNA mitochondria AhR binding and spindle organization. *Mutat Res* 713,18-31.

Healey, K., Smith, E. C., Wild, C. P., Routledge, M. N. (2006). The mutagenicity of urban particulate matter in an enzyme free system is associated with the generation of reactive oxygen species. *Mutation Research/Fundamental and Molecular Mechanisms of Mutagenesis* 602 (1-2), 1-6.

Iyer, D.R., Rhind, N. (2017). The intra-S checkpoint responses to DNA damage. *Genes* 8 (74), 1-25.

Lawal, A.O. (2017). Air particulate matter induced oxidative stress and inflammation in cardiovascular disease and atherosclerosis: The role of Nrf2 and AhR-mediated pathways. *Toxicol Lett.* 270, 88-95.

Leclercq, B., Happillon, M., Antherieu, S., Hardy, E.,M., Alleman, L.,Y., Grova, N., Perdrix, E., Appenzeller, B.,M., Lo Guidice, J.-M., Coddeville, P., Garçon, G. (2016). Differential responses of healthy and chronic obstructive pulmonary diseased human bronchial epithelial cells repeatedly exposed to air pollution-derived PM4. *Env. Poll.* 218, 1074-1088.

Leclercq, B., Platel, A., Antherieu, S., Alleman, L.Y., Hardy, E.M., Perdrix, E., Grova, N., Riffault, V., Appenzeller, B.M., Happillon, M., Neslany, F., Coddeville, P., Lo Guidice, J.-M., Garçon, G. (2017a). Genetic and epigenetic alterations in normal and sensitive COPD-diseased human bronchial epithelial cells repeatedly exposed to air pollution-derived $PM_{2.5}$. *Env. Poll.* 230, 163-177.

Leclercq, B., Alleman, L.Y., Perdrix, E., Riffault, V., Happillon, M., Strecker, A., Lo Guidice J.M., Garçon, G., Coddeville, P. (2017b). Particulate metal bioaccessibility in physiological fluids and cell culture media: Toxicological perspectives? *Env Res* 156, 148-157.

Leclercq, B., Kluza, J., Antherieu, S., Sotty, J., Alleman, L.Y., Perdrix, E., Loyens, A., Coddeville, P., Lo Guidice, J.M., Marchetti, P., Garçon, G. (2018). Air pollution-derived $PM_{(2.5)}$ impairs mitochondrial function in healthy and chronic obstructive pulmonary diseased human bronchial epithelial cells. *Environ Pollut.* 243(Pt B), 1434-1449.

Lepers, C., Dergham, M., Armand L., Billet, S., Verdin, A., Andr_e, V., Pottier, D., Courcot, D., Shirali, P., Sichel, F. (2014). Mutagenicity and clastogenicity of native airborne particulate matter samples collected under industrial urban or rural influence. Toxicol in Vitro 28, 866-874.

Liu, S., Cai, S., Chen, Y., Xiao, B., Chen, P., Xiang, X. D. (2016). The effect of pollutional haze on pulmonary function. *J. Thorac. Dis.* 8 (1), 41-56.

Longhin, E., Pezzolato, E., Mantecca, P., Holme, J.A., Franzetti, A., Camatini, M., Gualtieri, M. (2013). Season linked responses to fine and quasi-ultrafine Milan PM in cultured cells. *Toxicol. in vitro,* 27, 551-559.

Lonkar, P., Dedon, P.C. (2011). Reactive species and DNA damage in chronic inflammation: reconciling chemical mechanisms and biological fates. *Int J Cancer* 128 (9), 1999-2009.

Loomis, D., Huang, W., Chen, G. (2013). The International Agency for Research on Cancer (IARC) evaluation of the carcinogenicity of outdoor air pollution: focus on China. *Chinese J. Cancer* 33 (4), 189-196.

Loxham, M., Morgan-Walsh, R.J., Cooper, M.J., Blume, C., Swindle, R.J., Dennison, P.W., Howarth, P.H., Cassee, F.R., Teagle, D.A.H., Palmer, M.R., Davies, D.E. (2015). The effects on bronchial epithelial mucociliary cultures of coarse fine and ultrafine particulate matter from an underground railway station. Toxicol. Sci. 145 (1), 98-107.

Ma, Q. (2013). Role of Nrf2 in Oxidative Stress and Toxicity. *Annu Rev Pharmacol Toxicol.* 53, 401-426.

Massoud, R., Shihadeh, A., Roumie, M., Youness, M., Gerard, J., Saliba, N., Saliba, N. (2011). Intraurban variability of PM_{10} and $PM_{2.5}$ in an Eastern Mediterranean city. *Atmos. Res.* 101, 893-901.

MOEW. (2010). Policy Paper for the electricity sector, *H.E Gebran Bassil Ministry of Energy and Water.*

Nguyen, P.M., Park, M.S., Chow, M., Chang, J.H., Wrischnik, L., Chan, W.K., (2010). Benzo[*a*]pyrene increases the Nrf2 content by downregulating the Keap1 message. *Toxicol. Sci.* 116, 549-561.

Oh, M., Kim, H. R., Park, Y. J., Chung, K. H. (2011). Organic extracts of urban air pollution particulate matter ($PM_{2.5}$)-induced genotoxicity and oxidative stress in human lung bronchial epithelial cells (BEAS-2B cells). *Mutat. Res./Genetic Toxicol. Environ. Mutagen.* 723 (2), 142-151.

Park, C.H., Lee I.S., Grippo, P., Pandol, S.J., Gukovskaya, A.S., Edderkaoui, M. (2013) AKT kinase mediates the prosurvival effect of smoking compounds in pancreatic ductal cells. Pancreas. 2013; 42, 655-662.

Perrone, M. G., Gualtieri, M., Ferrero, L;, Lo Porto, C., Udisti, R., Bolzacchini, E., Camatini, M., (2010). Seasonal variations in chemical composition and *in vitro* biological effects of fine PM from Milan. Chemosphere 78 (11), 1368-1377.

Perrone, M.G., Gualtieri, M., Consonni, V., Ferrero, L., Sangiorgi, G., Longhin, E., Ballabio, D., Bolzacchini, E., Camatini, M. (2013). Particle size, chemical composition, seasons of the year and urban, rural or remote site origins as determinants of biological effects of particulate matter on pulmonary cells. *Environ Pollut.*, 176, 215-227.

Pui, D., Chen, S. C., Zuo, Z. (2014). $PM_{2.5}$ in China: Measurements, sources, visibility and health effects, and mitigation. *Particulogy 13*, 1-26.

Podhorecka, M., Skladanowski, A., Bozko, P. 52010). H2AX phosphorylation: its role in DNA damage response and cancer therapy. *J Nucleic Acids*. 2010: 1-9. (doi:10.4061/2010/920161)

Ravindra, K., Sokhi, R., Van Grieken, R. (2008). Atmospheric polycyclic aromatic hydrocarbons: source attribution, emission factors and regulation. . *Atmos. Environ. 42*, 2895-2921.

Saint-Georges, F., Abbas, I., Billet, S., Verdin, A., Gosset, P., Mulliez, P., Garcon, G. (2008). Gene expression induction of volatile organic compound and/or polycyclic aromatic hydrocarbon-metabolizing enzymes in isolated human alveolar macrophages in response to air- borne particulate matter ($PM_{2.5}$). *Toxicology , 244*, 220–230.

Saint-Georges, F, Garçon, G, Escande, F, Abbas, I, Verdin, A, Gosset, P, Mulliez, P, Shirali, P. (2009). Role of air pollution particulate matter ($PM_{2.5}$) in the occurrence of loss of heterozygosity in multiple critical regions of 3p chromosome in human epithelial lung cells (L132). *Toxicol. Lett.* 187, 172-179.

Saliba, N., El jam, F., El tayar, G., Obeid, W., Roumie, M. (2010). Origin and variability of particulate matter (PM_{10} and $PM_{2.5}$) mass concentrations over an Eastern Mediterranean city. *97*, 106-114.

Suzuki, M., Otsuki, A., Keleku-Lukwete, N., Yamamoto, M. (2016). Overview of redox regulation by Keap1–Nrf2 system in toxicology and cancer. *Curr Opinion Toxicol.* 1, 29-36.

Tu, W.Z., Li, B., Huang, B., Wang, Y., Liu, X.D., Guan, H., Zhang, S.M., Tang, Y., Rang, W.Q., Zhou, P.K. (2013). γH2AX foci formation in the absence of DNA damage: mitotic H2AX phosphorylation is mediated by the DNA-PKcs/CHK2 pathway. *FEBS Lett.* 587: 3437-3443.

US-EPA (2016); Revised air quality standards for particle pollution and updates to the air quality index (AQI).

Valavanidis, A., Vlachogianni, T., & Fiotakis, C. (2009). 8-hydroxy-2' -deoxyguanosine (8-OHdG): A critical biomarker of oxidative stress and carcinogenesis. *J Environ Sci Health C Environ Carcinog Ecotoxicol Rev., 27* (2), 120-139.

Van den Berg M., Birnbaum L.S., Denison M., De Vito M., Farland W., Feeley M., Fiedler H., Hakansson H., Hanberg A., Haws L., Rose M., Safe S., Schrenk D., Tohyama C., Tritscher A., Tuomisto J., Tysklind M.,

Walker N., Peterson R.E. (2006). The 2005 World Health Organization reevaluation of human and Mammalian toxic equivalency factors for dioxins and dioxin-like compounds. *Toxicol. Sci.* 93, 223-241

Wardyn, J.D., Ponsford, A.H., Sanderson, C.M. (2015). Dissecting molecular cross-talk between Nrf2 and NF-κB response pathways. *Biochem, Soc, Trans.* 43, 621-626.

Weber, S. A., Insaf, T. Z., Hall, E. S., Talblot, T. O., Huff, A. K. (2016). Assessing the impact of fine particulate matter ($PM_{2.5}$) on respiratory-cardiovascular chronic diseases in the New York City Metropolitan area using Hierarchical Bayesian Model estimates. *Environ. Res. 151,* 399-409.

Weissenberg, A., Sydlik, U., Peuschel, H., Schroeder, P., Schneider, M., Schins, R.P., Abel, J., Unfried, K. (2010). Reactive oxygen species as mediators of membrane-dependent signaling induced by ultrafine particles. *Free Radic Biol Med.* 49, 597-605.

WHO (2015) WHO Air quality guidelines for particulate matter, ozone, nitrogen dioxide and sulfur dioxide. WHO Air quality guidelines.

Wu, J., Shi, Y., Asweto, C.O., Feng, L., Yang, X., Zhang, Y., Hu, H., Duan, J., Sun, Z. (2017). Fine particle matters induce DNA damage and G2/M cell cycle arrest in human bronchial epithelial BEAS-2B cells. Environ Sci Pollut Res Int. 24 (32), 25071-25081.

Xiang, P., He, R., Liu, R., Li, K., Gao, P., Cui, X., Li, H.; Liu, Y.; Ma, L.Q. (2018). Cellular responses of normal (HL-7702) and cancerous (HepG2) hepatic cells to dust extract exposure . *Chemosphere 193*, 1189-1197.

Xing, Y., Xu, Y., Shi, M., Lian, Y. (2016). The impact of $PM_{2.5}$ on the human respiratory system . *J. Thoracic Dis., 8*, 69-74.

Zhang, Z., Yang, X., Wang, Y., Wang, X., Lu, H., Zhang, X., Xiao, X., Li, S., Wang, X., Wang, S.L. (2013). Cytochrome P450 2A13 is an efficient enzyme in metabolic activation of aflatoxin G1 in human bronchial epithelial cells. *Arch Toxicol*. 87, 1697-1707.

Zhou, B., Liang, G., Qin, H., Peng, X., Huang, J., Li, Q., Qing, L., Zhang, L., Chen, L., Ye, L., Niu, P., Zou, Y. (2014). p53-Dependent apoptosis induced in human bronchial epithelial (16-HBE) cells by $PM_{2.5}$ sampled from air in Guangzhou, China. *Toxicol Mech Methods*. 24 (8), 552-559.

Zhou W, Tian D, He J, Wang Y, Zhang L, Cui L, Jia L, Li L, Shu Y, Yu S (2016) Repeated PM2,5 exposure inhibits BEAS-2B cell P53 expression through ROS-Akt-DNMT3B pathway-mediated promoter hypermethylation, Oncotarget 7:20691-20703.

Zhou W, Tian D, He J, Zhang L, Tang X, Zhang L, Wang Y, Li L, Zhao J, Yuan X, Peng S (2017) Exposure scenario: Another important factor determining the toxic effects of $PM_{2.5}$ and possible mechanisms involved. Env Poll. 226:412-425

Zhuang, Z., Zhao, X., Wu, Y., Huang, R., Zhu, L., Zhang, Y., Shi, J. (2011). The anti-apoptotic effect of PI3K-Akt signaling pathway after subarachnoid hemorrhage in rats. *Ann Clin Lab Sci. Fall 41(4),* 364-372.

FIGURE LEGENDS

Figure 1: Adenosine triphosphate (ATP) concentrations in BEAS-2B cells and glucose-6-phosphate dehydrogenase (G6PD) activities in cell-free culture supernatants, 6, 24 and 72 h after their exposure to increasing concentrations of organic extract matter (OEM: 1, 3, 5, 15 and 30 μg $PM_{2.5}$-eq/cm^2). Results, normalized to control, are described by their means and their standard deviations (6 replicates for controls, and 6 replicates for exposed cells; Mann–Whitney U-test; *vs.* controls; a = p <0.05, b = p <0.01, c = p <0.001).

Figure 2: Gene and/or protein expression of nuclear factor erythroid 2–related factor 2 (NRF-2), heme oxygenase 1 (HMOX), NAD(P)H quinone dehydrogenase 1 (NQO1), superoxide dismutase (SOD), 8-isoprostane (8-Isop) and 8-hydroxy-2'-deoxyguanosine (8-OHdG) in BEAS-2B cells 6 and 24 h after their exposure to organic extract matter (OEM: 3, 15 and 30 μg $PM_{2.5}$-eq/cm^2) and B[*a*]P (25 μM). Results, normalized to control, are described by their means and their standard deviations (6 replicates for controls, and 6 replicates for exposed cells (Mann–Whitney U-test; *vs.* controls; a = p <0.05, b = p <0.01, c = p <0.001).

Figure 3: Concentrations of tumor necrosis factor (TNF-α), interleukin-1 beta (IL-1β), interleukin-6 (IL-6), interleukin-8 (IL-8), monocyte chemoattractant protein-1 (MCP-1), and interferon-gamma (IFN-γ), in the supernatants of BEAS-2B cells 6 and 24 h after their exposure to organic extract matter (OEM: 3, 15 and 30 μg $PM_{2.5}$-eq/cm^2) and B[*a*]P (25 μM). Results, normalized to control, are described by their means and their standard deviations (6 replicates for controls, and 6 replicates for exposed cells (Mann–Whitney U-test; *vs.* controls; a = p <0.05, b = p <0.01, c = p <0.001).

Figure 4: Gene expression of the *aryl hydrocarbon receptor* (*AHR*), *aryl hydrocarbon receptor nuclear translocator* (*ARNT*), *cytochrome P450 1A1* (*CYP1A1*) and *cytochrome P450 1B1* (*CYP1B1*) in BEAS-2B cells 6 and 24 h after their exposure to organic extract matter (OEM: 3, 15 and 30 μg $PM_{2.5}$-eq/cm^2) and B[*a*]P (25 μM). Results, normalized to control, are described by their means and their standard deviations (6 replicates for controls, and 6 replicates for exposed cells (Mann–Whitney U-test; *vs.* controls; a = p <0.05, b = p <0.01, c = p <0.001)

Figure 5: Concentrations of phosphorylated protein 53 (pP53), total protein 21 (P21), phosphorylated H2A histone family member X (H2AX), total mouse double minute 2 homolog (MDM-2), phosphorylated checkpoint kinase 1 (CHK-1), and phosphorylated checkpoint kinase 2 (CHK-2) in BEAS-2B cells in BEAS-2B cells 24 and 72 h after their exposure to organic extract matter (OEM: 3, 15 and 30 μg $PM_{2.5}$-eq/cm^2) and B[*a*]P (25 μM). Results, normalized to control, are described by their means and their standard deviations (6 replicates for controls, and 6 replicates for exposed cells (Mann–Whitney U-test; *vs.* controls; a = p <0.05, b = p <0.01, c = p <0.001)

Figure 6: Percentage of BEAS-2B cells in G1, S, and G2M cell cycle phases 24 and 72 h after their exposure to organic extract matter (OEM: 3, 15 and 30 μg $PM_{2.5}$-eq/cm^2) and B[*a*]P (25 μM). Results, normalized to control, are described by their means and their standard deviations (6 replicates for controls, and 6 replicates for exposed cells (Mann–Whitney U-test; *vs.* controls; a = p <0.05, b = p <0.01, c = p <0.001)

Figure 7: Concentrations of phosphorylated protein kinase B (AKT), phosphorylated c-Jun N-terminal kinase (JNK), phosphorylated Bcl-2-associated death promoter (BAD), phosphorylated B-cell lymphoma 2 (BCL-2), and phosphorylated Caspase-8 and 9, in BEAS-2B cells 6 and 24 h after their exposure to organic extract matter (OEM: 3, 15 and 30 μg $PM_{2.5}$-eq/cm^2) and B[*a*]P (25 μM). Results, normalized to control, are described by their means and their standard deviations (6 replicates for controls, and 6 replicates for exposed cells (Mann–Whitney U-test; *vs.* controls; a = p <0.05, b = p <0.01, c = p <0.001)

Figure 8: Underlying mechanisms involved in the toxicity of air pollution-derived organic extract matter (OEM) in BEAS-2B cells (8-Isop: 8-Isoprostaglandin, 8-OHdG: 8-hydroxy-2'-deoxyguanosine, AhR: aryl hydrocarbon receptor, CYP1A1: cytochrome P450 1A1, CYP1B1: cytochrome P450 1B1, G6PD: glucose-6-phosphate dehydrogenase, H2AX: phosphorylated H2A histone family member X, HMOX: heme oxygenase 1, NQO1: NAD(P)H quinone dehydrogenase 1, NRF-2: nuclear factor erythroid 2–related factor 2, PAH: polycyclic aromatic

hydrocarbon, pAKT: phosphorylated protein kinase B, pBAD: phosphorylated Bcl-2-associated death promoter, PCB: polychlorobiphenyl, PCDD: polychloro dibenzo-p-dioxin, PCDF: polychlorodibenzofuran, pCHK-1: phosphorylated checkpoint kinase 1, pCHK-2: phosphorylated checkpoint kinase 2, pP53: phosphorylated protein 53, ROS: reactive oxygen species, SOD: superoxide dismutase).

Figure S1: Location of sampling site (A and B) and the concerned recorded wind rose

Figure 1

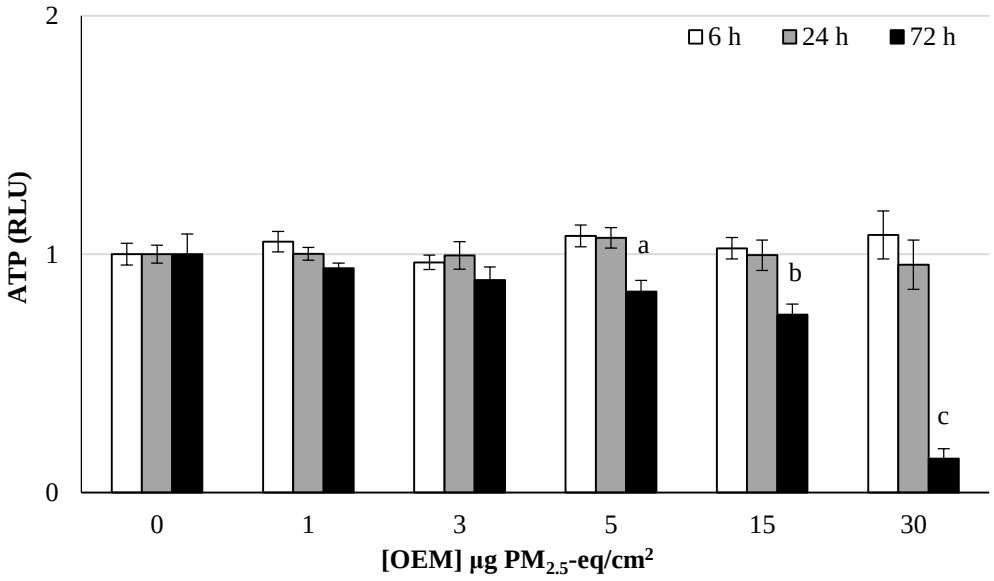
2
1
0
ATP (RLU)
6 h
24 h
72 h
a
b
c
0
1
3
5
15
30
[OEM] µg PM2.5-eq/cm2

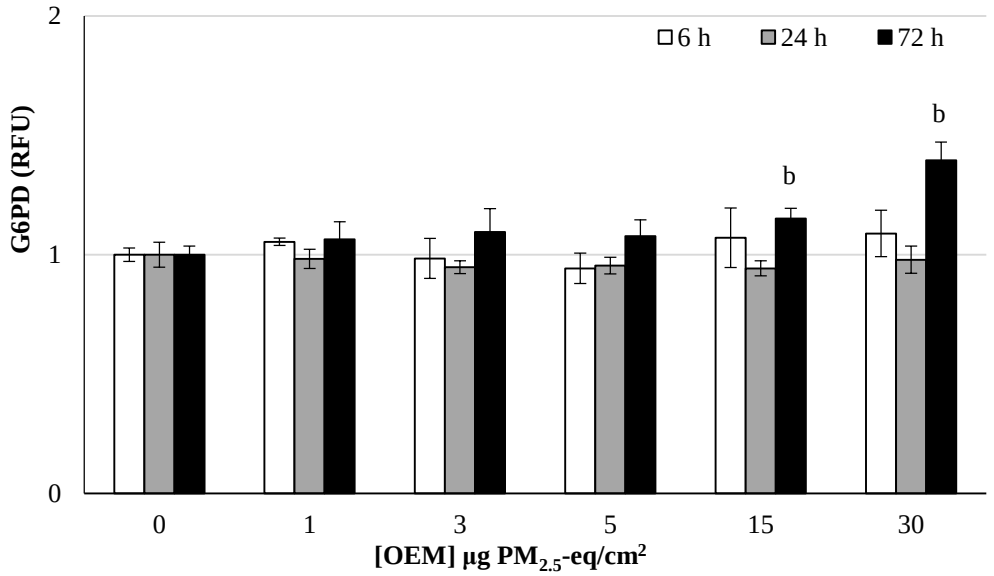
2
1
0
G6PD (RFU)
6 h
24 h
72 h
b
b
0
1
3
5
15
30
[OEM] µg PM2.5-eq/cm2

Figure 2

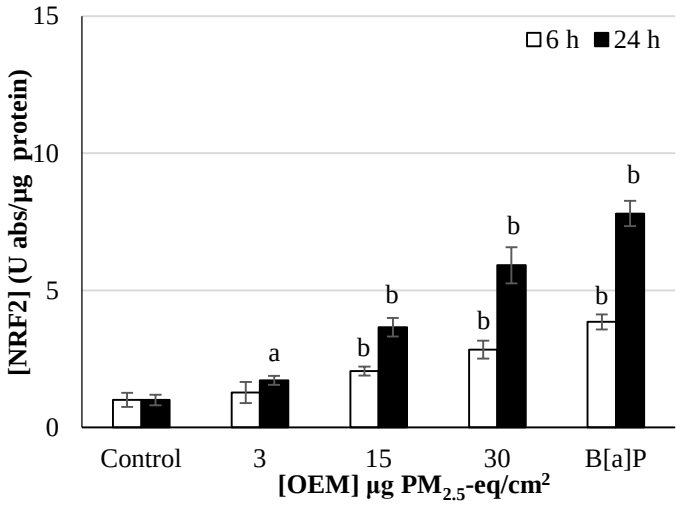
[NRF2] (U abs/µg protein)
6 h
24 h
Control
3
15
30
B[a]P
[OEM] µg PM2.5-eq/cm2

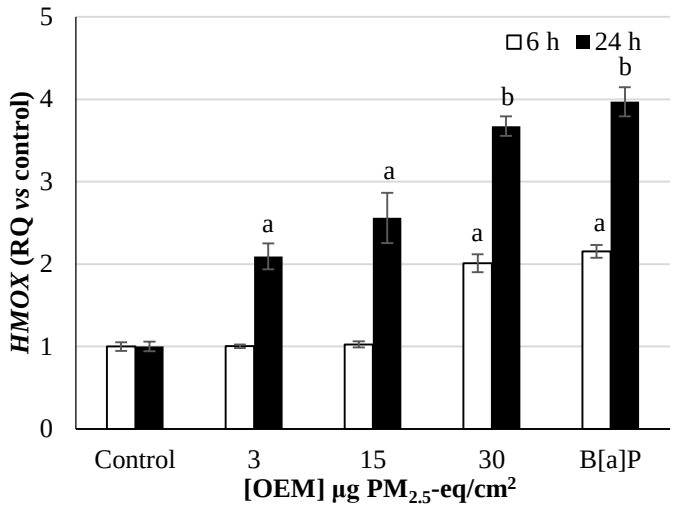
HMOX (RQ vs control)
6 h
24 h
Control
3
15
30
B[a]P
[OEM] µg PM2.5-eq/cm2

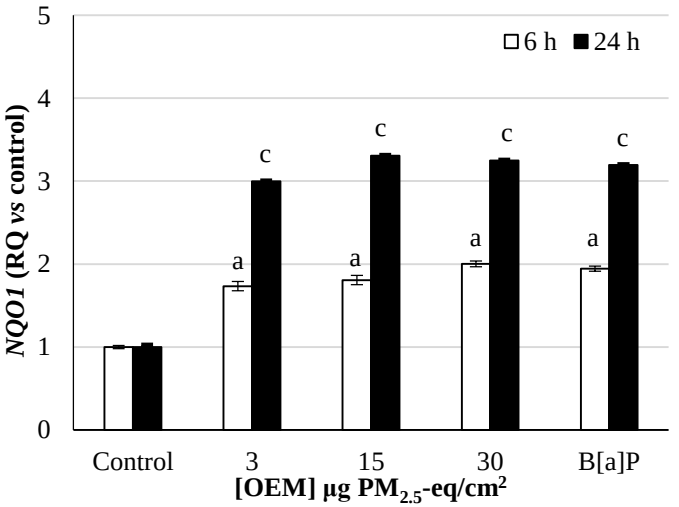
NQO1 (RQ vs control)
6 h
24 h
Control
3
15
30
B[a]P
[OEM] µg PM2.5-eq/cm2

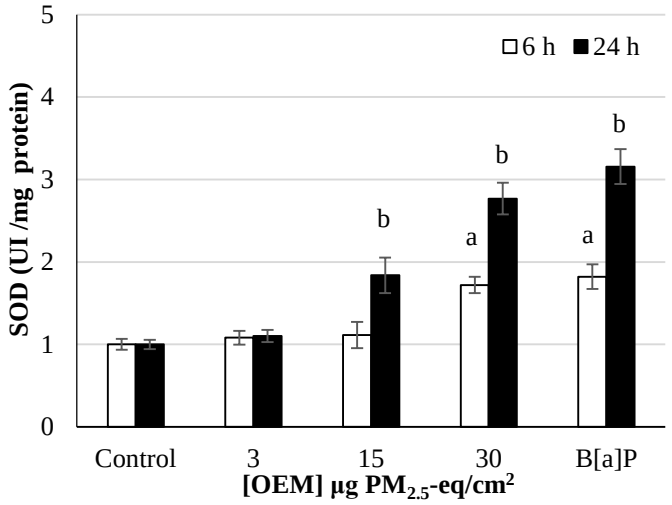
SOD (UI /mg protein)
6 h
24 h
Control
3
15
30
B[a]P
[OEM] µg PM2.5-eq/cm2

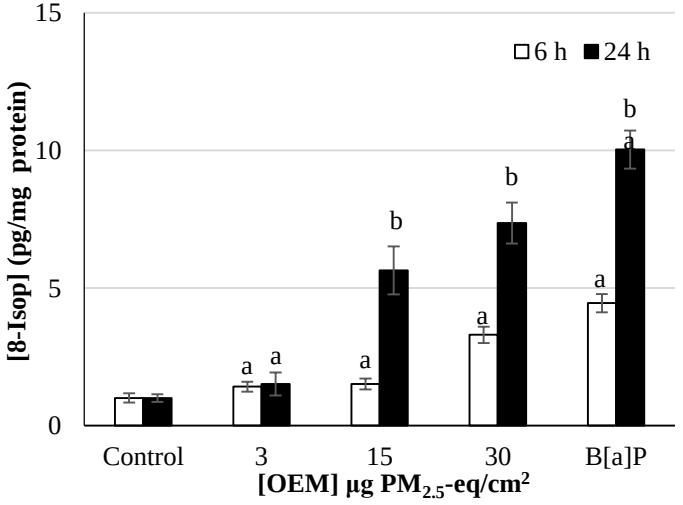
[8-Isop] (pg/mg protein)
6 h
24 h
Control
3
15
30
B[a]P
[OEM] µg PM2.5-eq/cm2

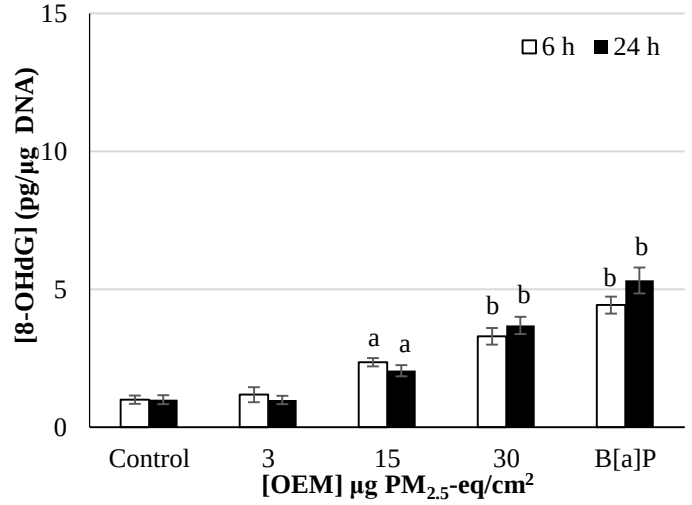
[8-OHdG] (pg/µg DNA)
6 h
24 h
Control
3
15
30
B[a]P
[OEM] µg PM2.5-eq/cm2

Figure 3

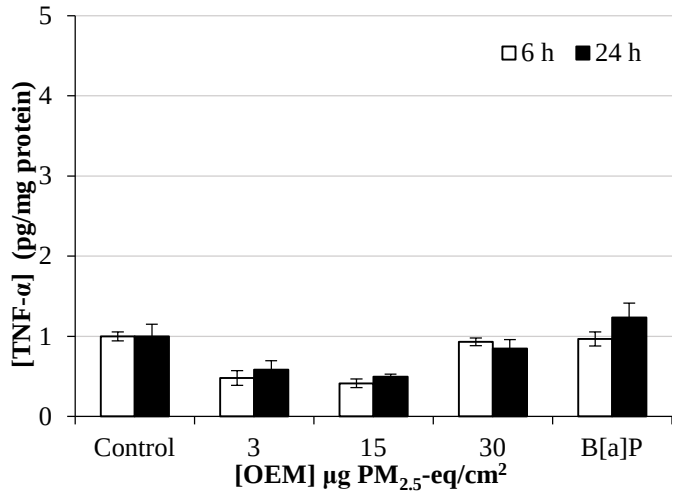
[TNF-α] (pg/mg protein)
6 h
24 h
Control
3
15
30
B[a]P
[OEM] µg PM2.5-eq/cm2

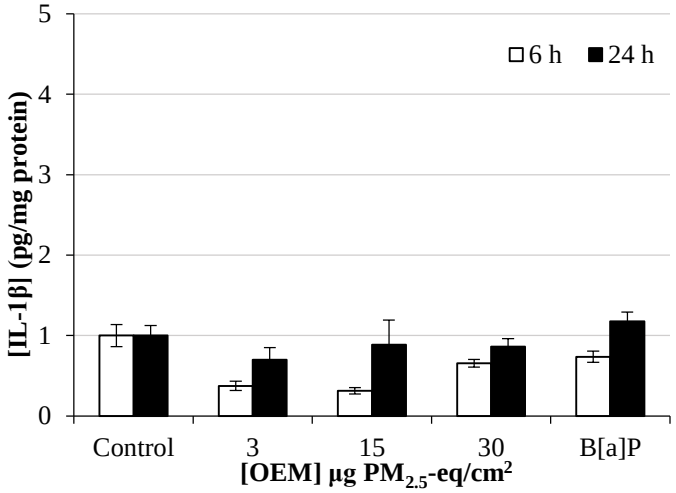
[IL-1β] (pg/mg protein)
6 h
24 h
Control
3
15
30
B[a]P
[OEM] µg PM2.5-eq/cm2

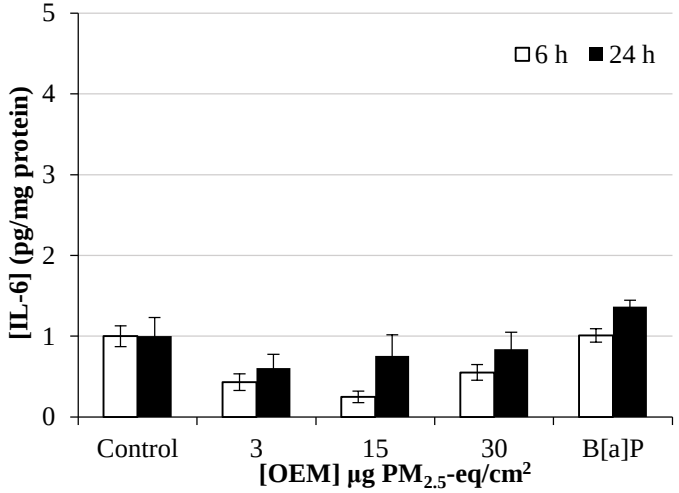
[IL-6] (pg/mg protein)
6 h
24 h
Control
3
15
30
B[a]P
[OEM] µg PM2.5-eq/cm2

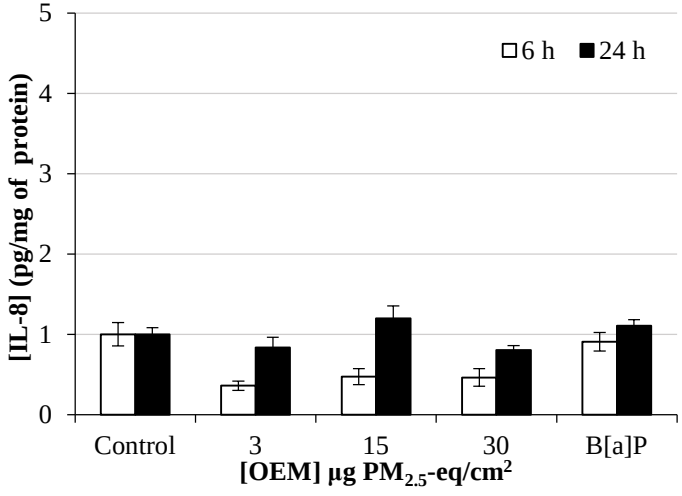
[IL-8] (pg/mg of protein)
6 h
24 h
Control
3
15
30
B[a]P
[OEM] µg PM2.5-eq/cm2

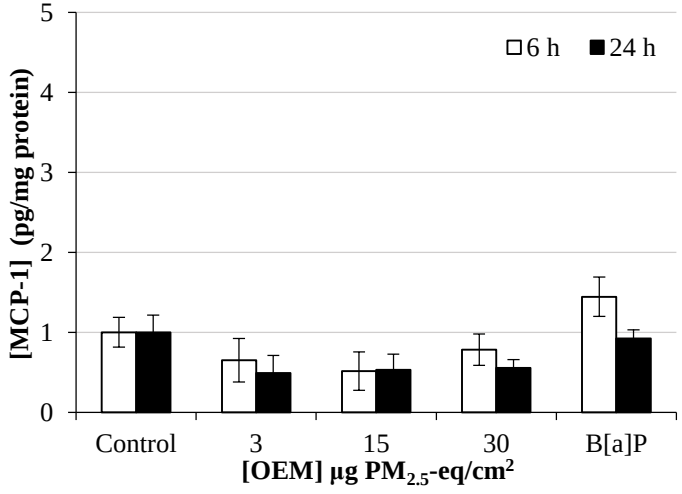
[MCP-1] (pg/mg protein)
6 h
24 h
Control
3
15
30
B[a]P
[OEM] µg PM2.5-eq/cm2

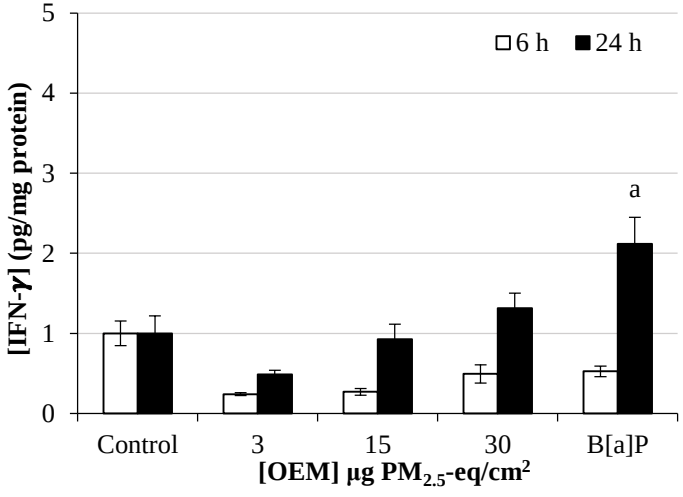
[IFN-γ] (pg/mg protein)
6 h
24 h
a
Control
3
15
30
B[a]P
[OEM] µg PM2.5-eq/cm2

Figure 4

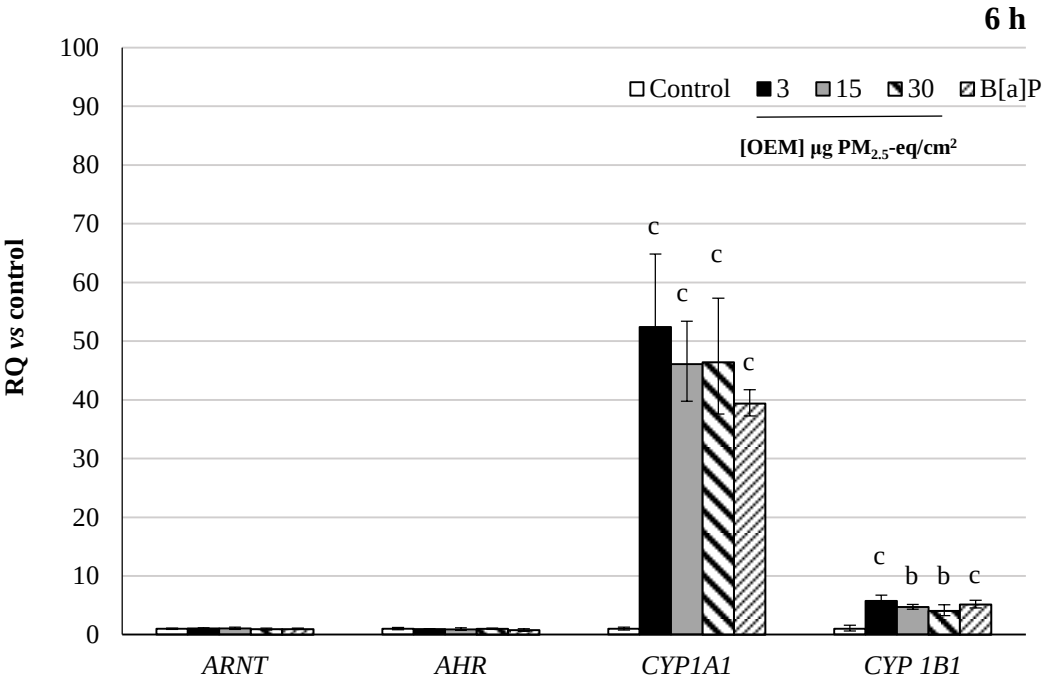
6 h
RQ vs control
Control
3
15
30
B[a]P
[OEM] µg PM2.5-eq/cm2
ARNT
AHR
CYP1A1
CYP 1B1

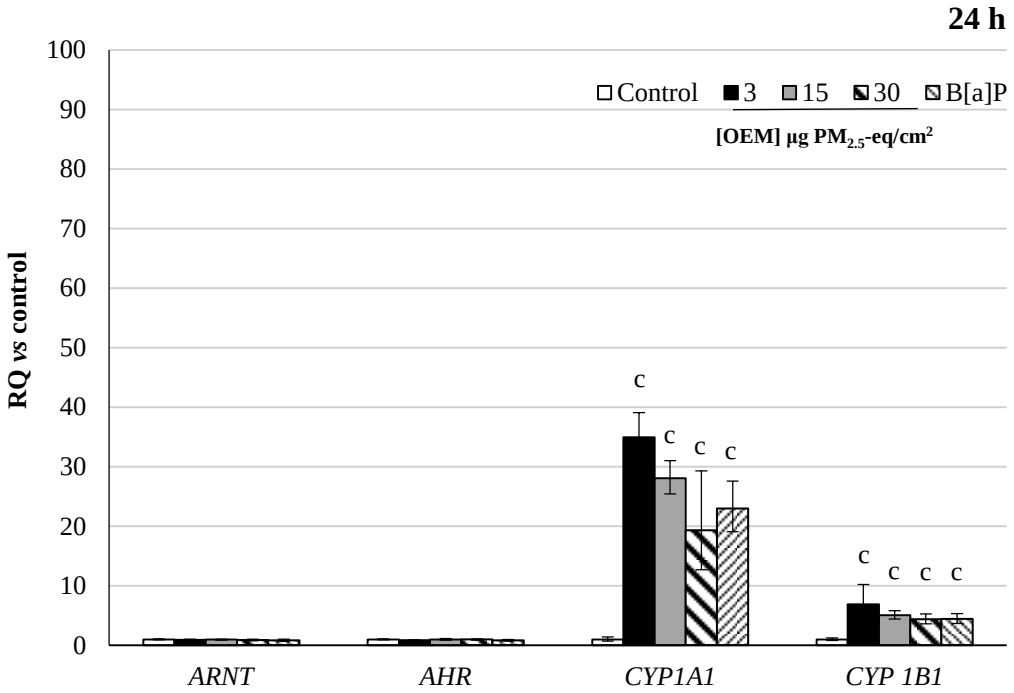
24 h
RQ vs control
Control
3
15
30
B[a]P
[OEM] µg PM2.5-eq/cm2
ARNT
AHR
CYP1A1
CYP 1B1

Figure 5

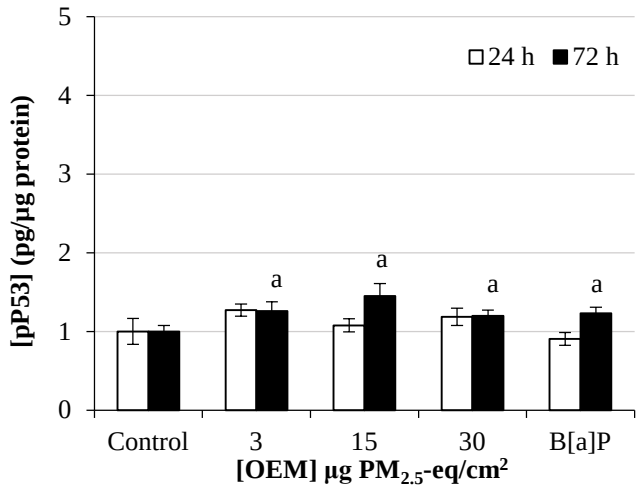
24 h
72 h
[pP53] (pg/µg protein)
a
a
a
a
Control
3
15
30
B[a]P
[OEM] µg PM2.5-eq/cm2

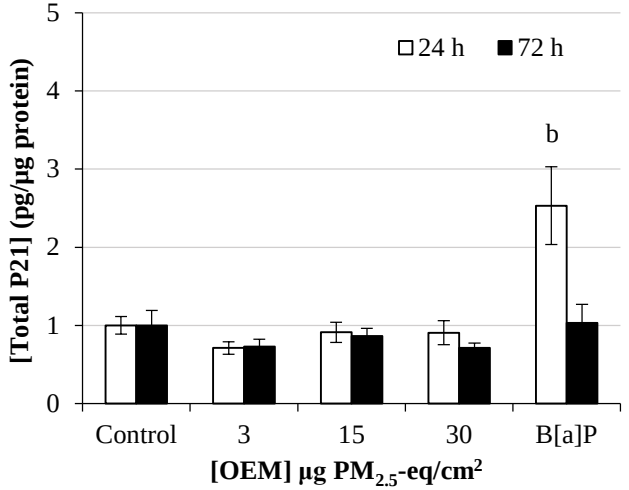
24 h
72 h
[Total P21] (pg/µg protein)
b
Control
3
15
30
B[a]P
[OEM] µg PM2.5-eq/cm2

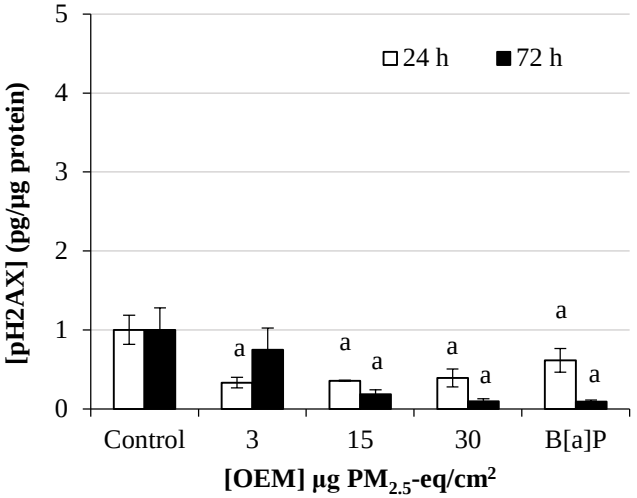
24 h
72 h
[pH2AX] (pg/µg protein)
a
a
a
a
a
a
a
Control
3
15
30
B[a]P
[OEM] µg PM2.5-eq/cm2

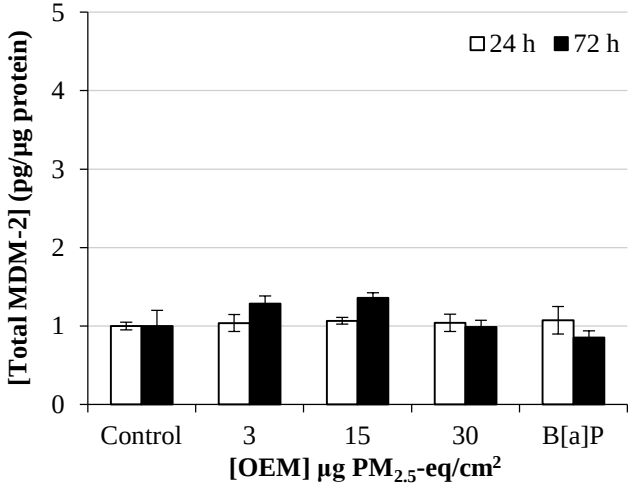
24 h
72 h
[Total MDM-2] (pg/µg protein)
Control
3
15
30
B[a]P
[OEM] µg PM2.5-eq/cm2

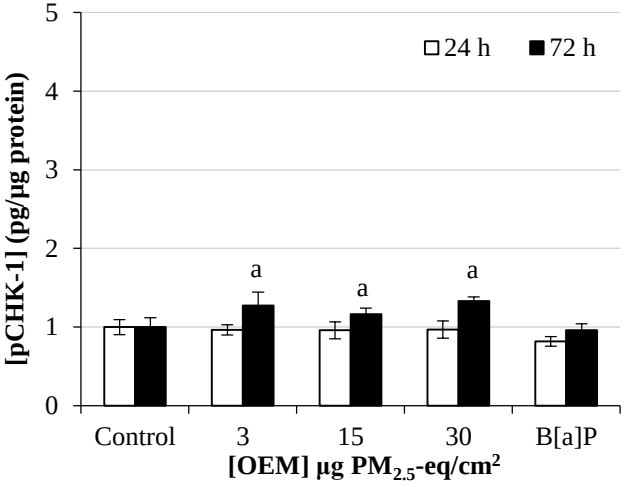
24 h
72 h
[pCHK-1] (pg/µg protein)
a
a
a
Control
3
15
30
B[a]P
[OEM] µg PM2.5-eq/cm2

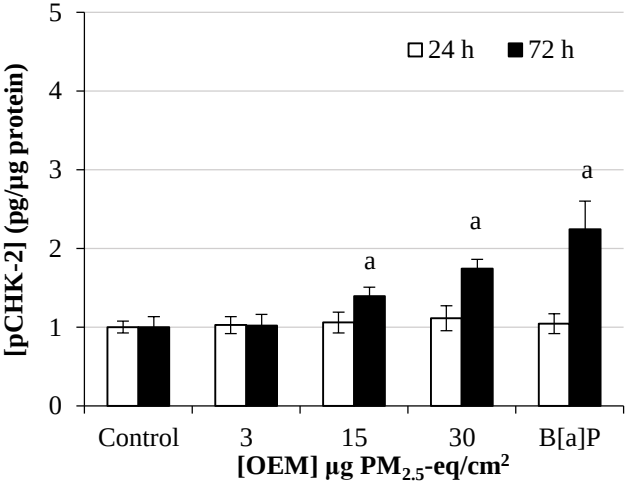
24 h
72 h
[pCHK-2] (pg/µg protein)
a
a
a
Control
3
15
30
B[a]P
[OEM] µg PM2.5-eq/cm2

Figure 6

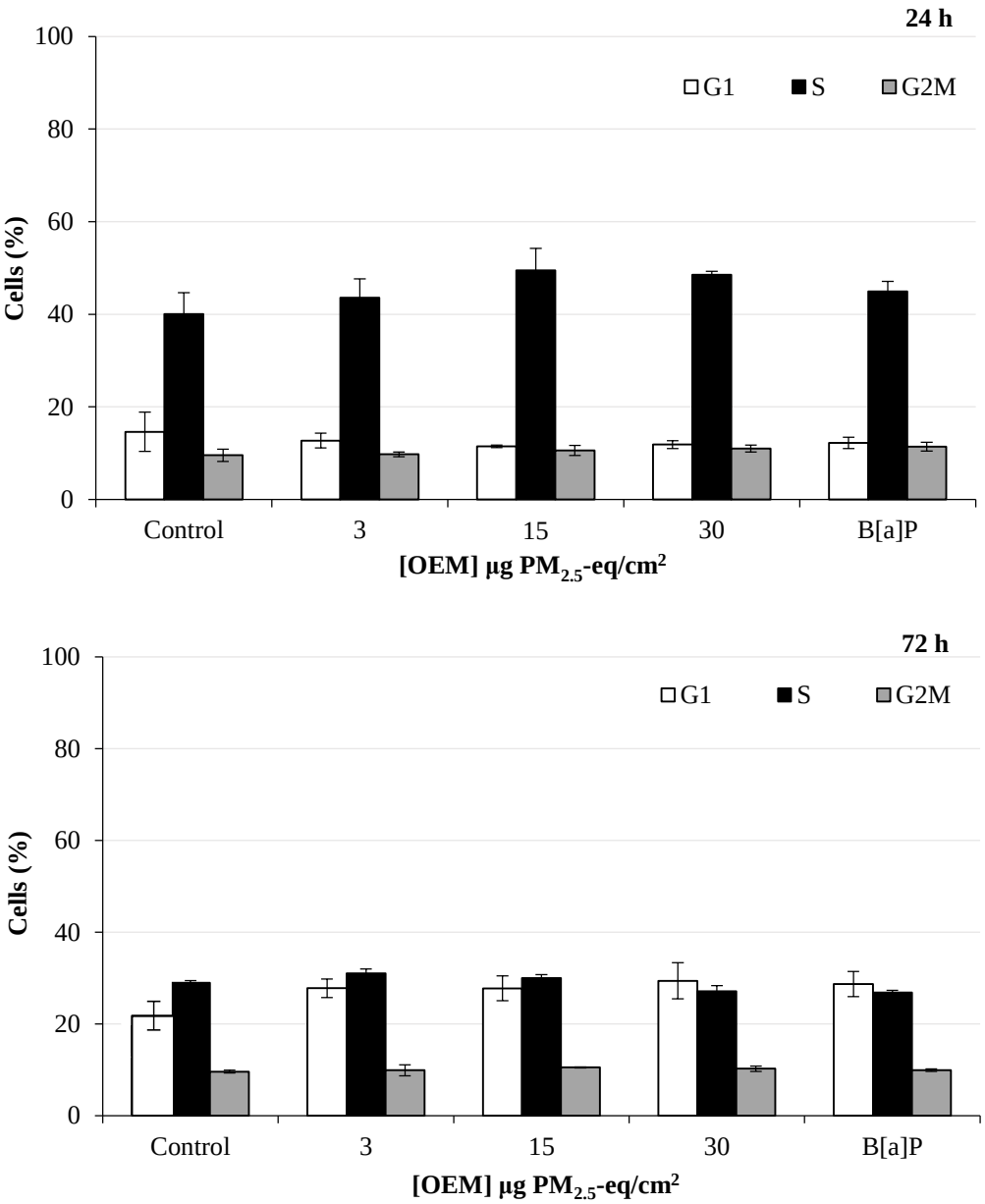
24 h
100
80
60
40
20
0
Cells (%)
G1
S
G2M
Control
3
15
30
B[a]P
[OEM] µg PM2.5-eq/cm2
72 h
100
80
60
40
20
0
Cells (%)
G1
S
G2M
Control
3
15
30
B[a]P
[OEM] µg PM2.5-eq/cm2

Figure 7

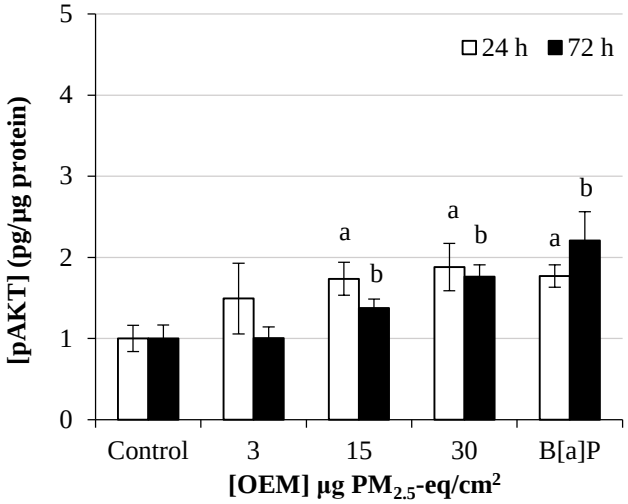
24 h
72 h
[pAKT] (pg/µg protein)
0
1
2
3
4
5
a
b
a
b
a
b
Control
3
15
30
B[a]P
[OEM] µg PM2.5-eq/cm2

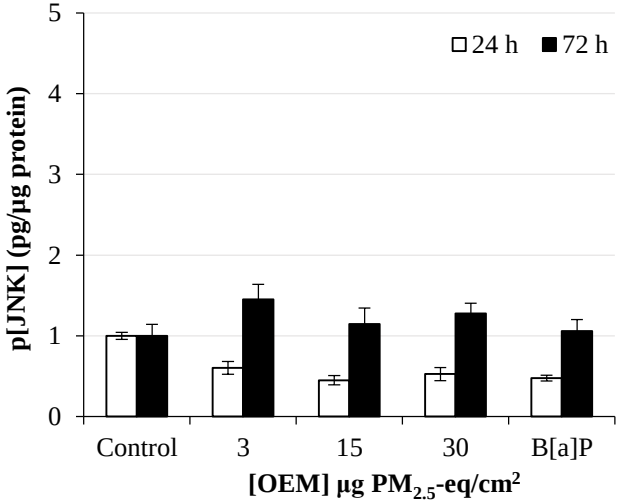
24 h
72 h
p[JNK] (pg/µg protein)
0
1
2
3
4
5
Control
3
15
30
B[a]P
[OEM] µg PM2.5-eq/cm2

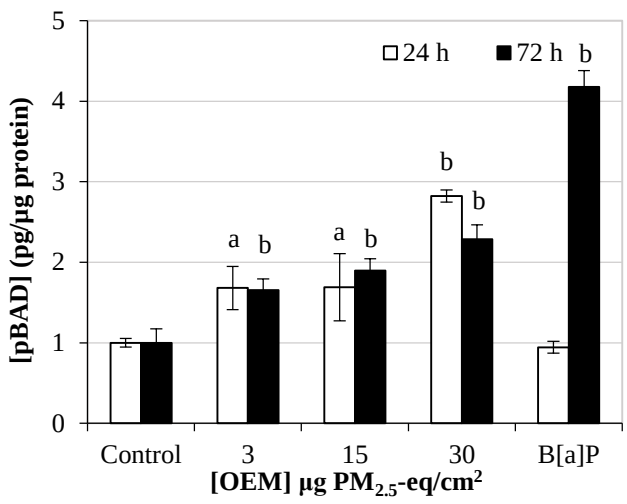
24 h
72 h
[pBAD] (pg/µg protein)
0
1
2
3
4
5
a
b
a
b
b
b
Control
3
15
30
B[a]P
[OEM] µg PM2.5-eq/cm2

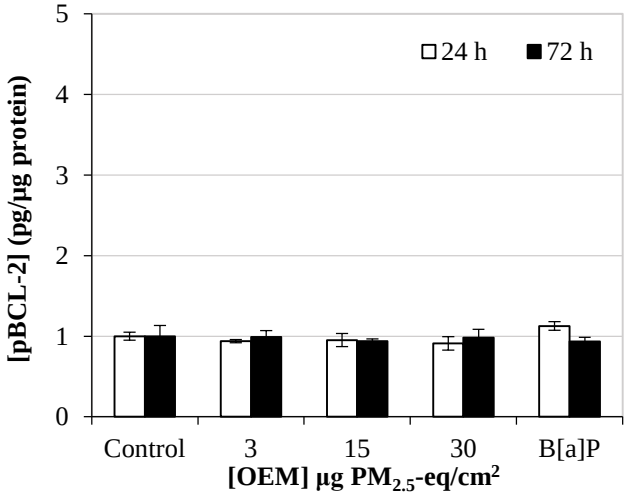
24 h
72 h
[pBCL-2] (pg/µg protein)
0
1
2
3
4
5
Control
3
15
30
B[a]P
[OEM] µg PM2.5-eq/cm2

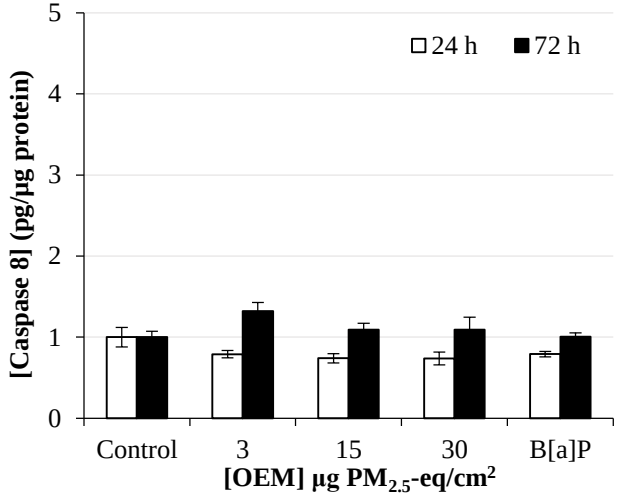
24 h
72 h
[Caspase 8] (pg/µg protein)
0
1
2
3
4
5
Control
3
15
30
B[a]P
[OEM] µg PM2.5-eq/cm2

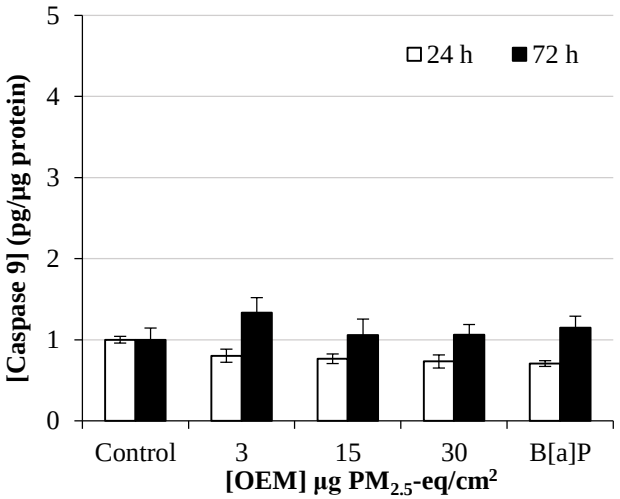
24 h
72 h
[Caspase 9] (pg/µg protein)
0
1
2
3
4
5
Control
3
15
30
B[a]P
[OEM] µg PM2.5-eq/cm2

Figure 8

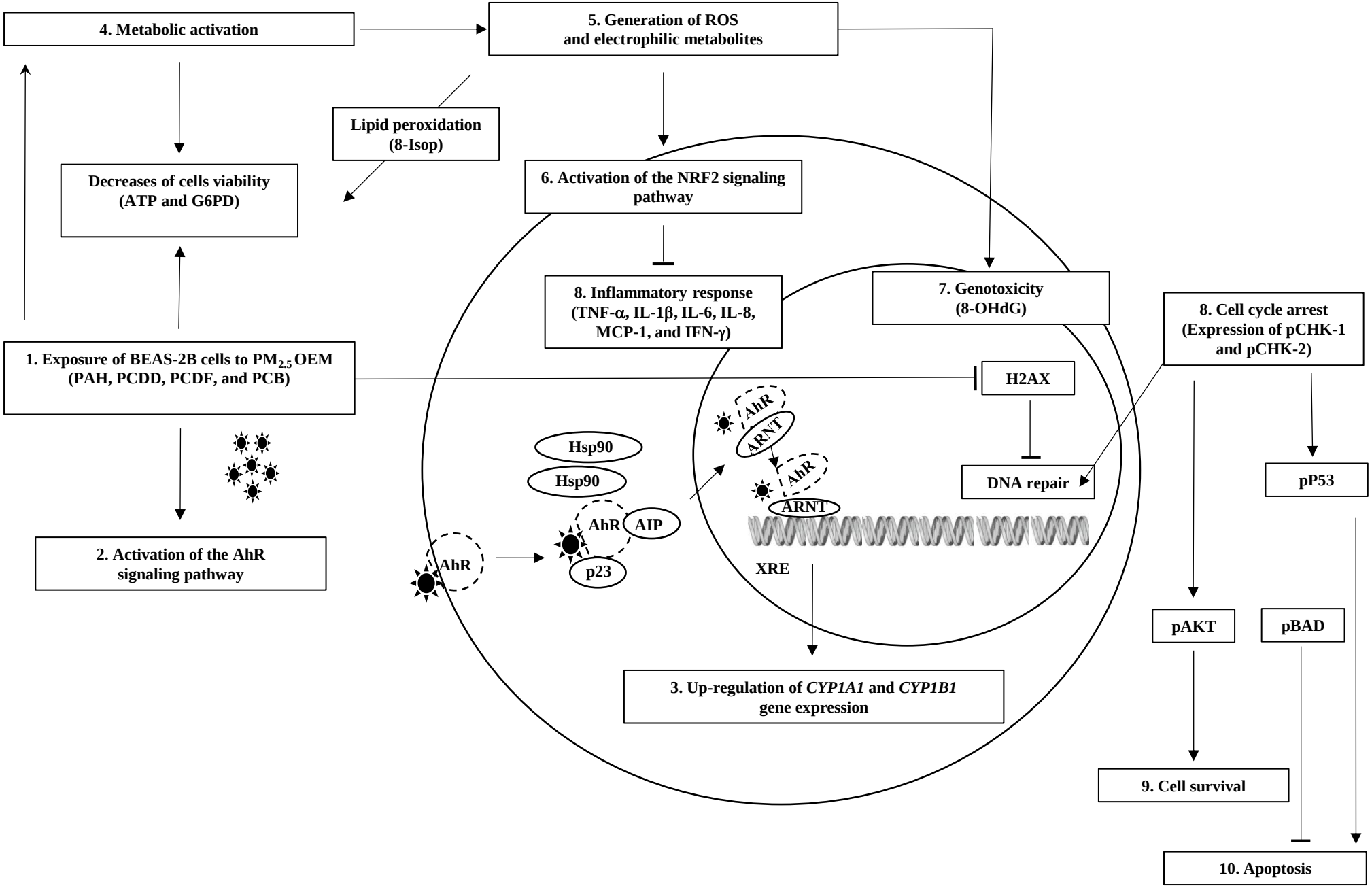
4. Metabolic activation
5. Generation of ROS and electrophilic metabolites
Lipid peroxidation (8-Isop)
Decreases of cells viability (ATP and G6PD)
6. Activation of the NRF2 signaling pathway
8. Inflammatory response (TNF-α, IL-1β, IL-6, IL-8, MCP-1, and IFN-γ)
7. Genotoxicity (8-OHdG)
8. Cell cycle arrest (Expression of pCHK-1 and pCHK-2)
1. Exposure of BEAS-2B cells to PM2.5 OEM (PAH, PCDD, PCDF, and PCB)
H2AX
DNA repair
pP53
Hsp90
Hsp90
AhR
AIP
p23
AhR
AhR
ARNT
AhR
ARNT
XRE
2. Activation of the AhR signaling pathway
3. Up-regulation of CYP1A1 and CYP1B1 gene expression
pAKT
pBAD
9. Cell survival
10. Apoptosis

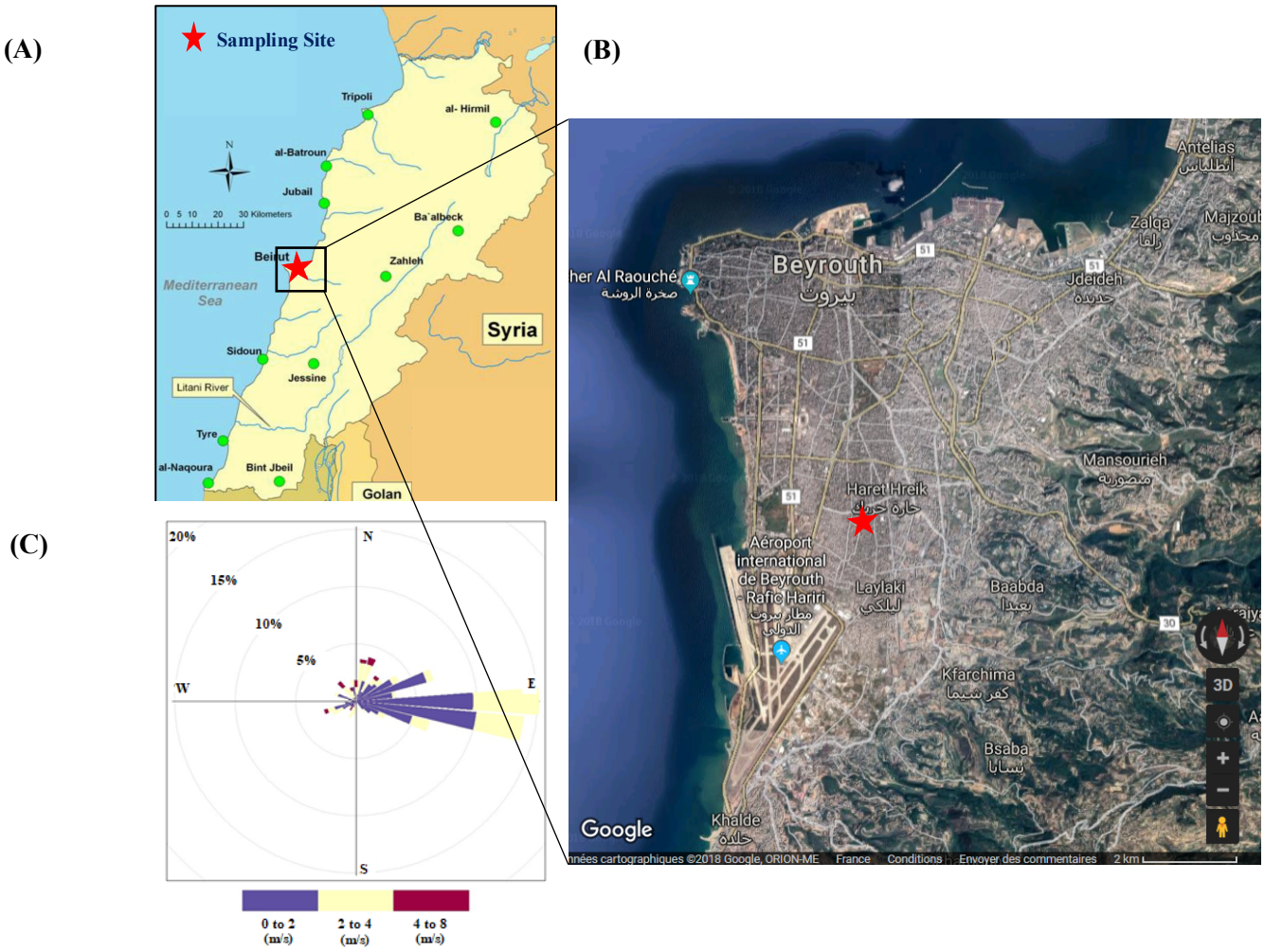

Figure S1: Location of sampling site (A and B) and the concerned recorded wind rose (C)

Table 1: Polycyclic aromatic hydrocarbons (PAH) concentrations in the ambient $PM_{2.5}$ collected in Beirut (Lebanon).

Congener [a]	**Concentration (µg/g)**	**Concentration (pg/m^3)**
NAP	2.7	131
ACY	4.5	218
ACE	2.3	112
FLU	<0.2	<11
PHE	9.6	458
ANT	2.8	134
FLT	15.4	736
PYR	25.9	1243
B[*a*]A	25.7	1231
CHR	28.8	1379
B[*b*]F	31.7	1519
B[*k*]F	8.2	394
B[*a*]P	12.9	618
D[*ah*]A	<0.2	<11
I[*cd*]P	10.3	495
B[*ghi*]P	20.6	989
Total PAH	**202**	**9655**

[a] Naphthalene: NAP, Acenaphthylene: ACY, Acenaphthene: ACE, Fluorene: FLU, Phenanthrene: PHE, Anthracene: ANT, Fluoranthene: FLT, Pyrene: PYR, Benz[*a*]anthracene: B[*a*]A, Chrysene: CHR, Benzo[*b*]fluoranthene: B[*b*]F, Benzo[*k*]fluoranthene: B[*k*]F, Benzo[*a*]pyrene: B[*a*]P, Dibenz[*ah*]anthracene: D[*ah*]A, Indeno[*123cd*]pyrene: I[*cd*]P, Benzo[*ghi*]perylene: B[*ghi*]P

Table 2: PolyChloro Dibenzo-p-Dioxins (PCDD), PolyChloroDibenzoFurans (PCDF) and PolyChloroBiphenyls (PCB) concentrations in the ambient $PM_{2.5}$ in Beirut (Lebanon)

Congener [a]	**Concentration (pg/g)**	**Concentration (fg/m^3)**
2,3,7,8 TCDD	39	2
1,2,3,7,8 PeCDD	184	9
1,2,3,4,7,8 HxCDD	220	11
1,2,3,6,7,8 HxCDD	480	23
1,2,3,7,8,9 HxCDD	380	18
1,2,3,4,6,7,8 HpCDD	3,170	152
OCDD	5,114	245
Total PCDD	**9,587**	**459**
2,3,7,8 TCDF	401	20
1,2,3,7,8 PeCDF	431	20
2,3,4,7,8 PeCDF	919	40
1,2,3,4,7,8 HxCDF	1,076	50
1,2,3,6,7,8 HxCDF	983	50
2,3,4,6,7,8 HxCDF	1,341	50
1,2,3,7,8,9 HxCDF	304	10
1,2,3,4,6,7,8 HpCDF	3933	200
1,2,3,4,7,8,9 HpCDF	477	20
OCDF	2,390	100
Total PCDF	**12,255**	**560**
PCB81	214	10
PCB77	791	38
PCB123	156	7
PCB118	7,330	351
PCB114	156	7
PCB105	4,213	202
PCB126	483	23
PCB167	2,124	102
PCB156	2,573	123
PCB157	317	15
PCB169	279	13
PCB189	1,182	57
Total DL-PCB	**19,818**	**949**

[a] Tera- (T), Penta- (Pe), Hexa- (Hx), Hepta- (Hp), and Octa (O)-chlorinated Dibenzo-p-Dioxin (PCDD) and Dibenzo-Furans (PCDF). Dioxin-Like PolyChlorinated Biphenyls: DL-PCB.

Table 3: PAH ratios used as source indicators

Diagnosis Ratio [a]	Literature [b]		Current Study
	Values	Sources	
I[cd]P/(I[cd]P + B[*ghi*]P)	0.18	Gasoline	0.33
	0.37	Diesel	
	0.56	Coal	
	0.62	Wood burning	
	0.35-0.70	Diesel emissions	
B[*a*]P/(B[*a*]P + CHR)	0.5	Diesel	0.3
	0.73	Gasoline	
B[*b*]F/B[*k*]F	<0.5	Diesel	3.8
B[*a*]P/B[*ghi*]P	0.5-0.6	Traffic emission	0.6
	>1.25	Brown coal	
PYR/B[*a*]P	≈10	Diesel Engine	2
	≈1	Gasoline engine	
FLT/PYR	0.6	Vehicular emissions	0.6

[a] Fluoranthene: FLT, Pyrene: PYR, Chrysene: CHR, Benzo[*b*]fluoranthene: B[*b*]F, Benzo[*k*]fluoranthene: B[*k*]F, Benzo[*a*]pyrene: B[*a*]P, Indeno[*123cd*]pyrene: I[*cd*]P, Benzo[*ghi*]perylene: B[*ghi*]P
[b] Adapted from Ravindra *et al.* (2008) and Borgie *et al.* (2015a)

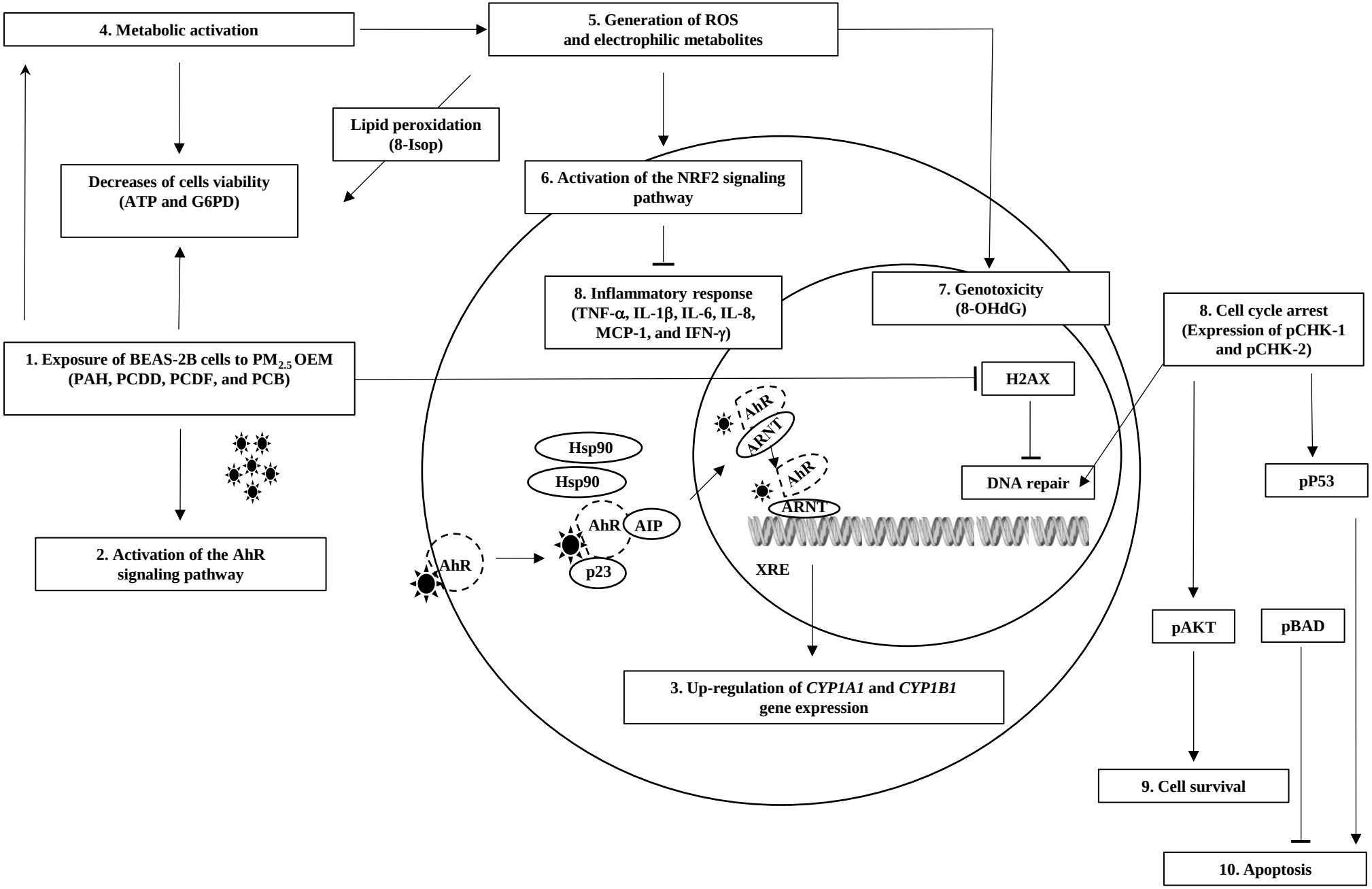
4. Metabolic activation
5. Generation of ROS
and electrophilic metabolites
Lipid peroxidation
(8-Isop)
Decreases of cells viability
(ATP and G6PD)
6. Activation of the NRF2 signaling
pathway
8. Inflammatory response
(TNF-α, IL-1β, IL-6, IL-8,
MCP-1, and IFN-γ)
7. Genotoxicity
(8-OHdG)
8. Cell cycle arrest
(Expression of pCHK-1
and pCHK-2)
1. Exposure of BEAS-2B cells to PM2.5 OEM
(PAH, PCDD, PCDF, and PCB)
H2AX
Hsp90
Hsp90
AhR
AIP
p23
AhR
AhR
ARNT
AhR
ARNT
DNA repair
pP53
XRE
2. Activation of the AhR
signaling pathway
3. Up-regulation of CYP1A1 and CYP1B1
gene expression
pAKT
pBAD
9. Cell survival
10. Apoptosis